Response to reviews and comments on "*An aerosol activation metamodel of v1.2.0 of the pyrcel cloud parcel model: Development and offline assessment for use in an aerosol-climate model*"

We would like to think the reviewers for their thoughtful, thorough, and helpful suggestions and feedback on our manuscript. We appreciate the reviewers' recognition of the potential for emulator approaches, such as the one we discuss in our manuscript, to improve parameterizations of aerosol-cloud interactions in global models, and have made efforts (as documented below) to address the additional questions and issues they identified pertaining to the manuscript.

Below, we respond to each of the "General" and "Specific" comments from the three reviewers, and recorded the actions taken in response to the "Minor" comments provided. We first respond generally to three additional, common "General" comments raised by all three reviewers here:

1. All three reviewers requested additional details on the computational expense of the metamodels, and more information on how they could be used in global models. Up to and during the review of this manuscript, we completed the implementation of a set of our activation metamodels into a global climate mode. Although we defer the discussion of the full impacts of these schemes on the simulated climate to a future manuscript currently *in preparation*, we are able to include a discussion of the impact the emulators have on the computational expense of the global model, compared with the other activation schemes we consider in this manuscript. This discussion has been added to the concluding section of the manuscript. In short, 3 of the 4 activation models yield negligible impact on the performance of MARC versus the reference ARG implementation. The MBN scheme increases the computational expense by about 7%; the 4th-order gCCN scheme incurs an increase of just 3%.

2. All three reviewers expressed concern that the manuscript was much too long, did not explicitly clarify its differences with Rothenberg and Wang (2016), and did not focus narrowly enough on the develop and evaluation of the metamodels. To address these points, we have re-written the Introduction nearly in its entirety to exclude historical details of activation parameterization development better recounted elsewhere (e.g. in Ghan et al. (2011)), and consolidated the discussion in Sections 2 and 3 into a single section entitled "Emulation of aerosol activation". Furthermore, we have worked to eliminate the reproduction of material available in Rothenberg and Wang (2016), opting to refer the reader there for details on the parcel model used here and on the polynomial chaos expansion technique.

3. All three reviewers included comments on redundancies in Section 2 and the iterative activation calculations. As mentioned previously, we have consolidated this Sections 2 and 3 and streamlined the discussion in both. Where possible, we have tried to include additional references to justify our decisions on how to exclude particular aerosol modes. Overall, we still feel it is important to include this discussion in the manuscript; a key difficulty in employing emulators and other statistical approaches to study physical processes and to develop parameterizations is the "curse of dimensionality," where increasing the number of important parameters tends to greatly increase the expense of building and evaluating a given emulator or statistical model. A critical component of such an effort, then, is rigorously searching for reduced sets of parameters to use in building the statistical models, often referred to as "feature extraction" in the machine learning community or otherwise "dimensionality reduction". Although there is a large literature on algorithms and automatic ways to accomplish this, these techniques often use a brute-force or exhaustive search approach. Our iterative calcu-

lations are the result of attempting to build a physically-informed algorithm for approaching feature extraction, and we hope that such an approach will be informative for researchers who pursue similar lines of study in the future. Therefore, we have tried to retain at least a limited discussion of the iterative calculations and results in the revised manuscript.

The remaining reviewers' comments are addressed below. We have made our best effort to address each individual comment in the sections labeled by the reviewers (General/Specific/Major/Minor/Technical comments, where denoted), and in the same order/numbering as they were presented. For clarity, we have included a summary of the reviewer's comment **in bold** before each response. Although this resulting document is somewhat long, we hope it fully documents our attempts to incorporate all of the thoughtful critiques provided by the reviewers and outlines our planned revisions to the manuscript.

Reviewer #1

General Comments

- **Lengthy historical introduction**

  We have opted to extensively re-write the introduction to streamline the introduction, referring the reader to other literature for more information. The new introduction is focused on the critical literature most pertinent to the development of our new method and parameterization.

- **Failure to focus on description of emulator development and related work**

  We have included discussion of the noted literature (Partridge et al. (2011) and Carslaw et al. (2013)) and other work on emulation as applied to atmospheric and climate processes, and made an effort to place this new work in that appropriate context. We have also worked to reduce the duplication of details already available in Rothenberg and Wang (2016).

- **GCCN**

  Although the focus of this manuscript is not on analyzing the impacts of GCCN on the accuracy of activation calculations in general, we did wish to understand how their inclusion/exclusion could influence the relative performance of our metamodels. We agree that this was not sufficiently introduced in the manuscript, and have added a brief discussion on how the presence of GCCN impacts aerosol activation in the introduction. Additionally, we added some clarifying remarks where the separate "main" and "GCCN" schemes are introduced in the manuscript to better highlight our motivation for training two separate emulators.

- **Path forward/computational cost**

  We defer the reviewer to our comments at the beginning of this document. We also include brief remarks in the conclusion of the manuscript discussing our implementation in the global model and its implications for future work.

- **Testing of activation schemes**

  We agree with the reviewer that, in fact, activation schemes have been tested against complex aerosol distributions from a variety of tools, including GCMs and CTMs. However, we stress that our remarks about testing the schemes refers more-so to inter-comparisons of different

activation parameterizations. Since the comprehensive review of Ghan et al. (2011), few works have looked at how different activation schemes perform when coupled to the same host model, or using the same set of complex aerosol size distributions. In order to more accurately represent the historical work on this issue, we've amended some of our comments on this topic in the manuscript, especially in the Introduction (e.g. the first *Specific Comment* below).

Specific Comments

The following responses match exactly to each of the comments provided by the reviewer, in the order provided. We have included reference line numbers (used in the review) to help keep track of which comment is which, where possible.

- We've rephrased **P3/L33** following the final *General Comment* above and the reviewer's comment
- Section 2 has been entirely re-written, and consolidated with Section 3.
- **P6/L19**: Removed
- **Figure 2**: We've revised our presentation of the aerosol size distribution parameters, and have replaced the original Figure 2 with a plot featuring PDFs of those parameters. This complements Table 2 and our discussion of the emulator approach later in the manuscript.
- **Section 2.2**: Replaced and consolidated with Section 3
- **Section 2.3**: Replaced and consolidated with Section 3. In the revised manuscript we have greatly shortened the discussion of the iterative procedure.
- **P7/L31**: Re-phrased and worked differently as part of the shortening mentioned previously.
- **P8/L13**: Removed, similarly to the previous comment.
- **P8/L10-30**: Removed, similarly to the previous comment. Reviewer #2 raised a similar concern about our discussion of the mechanism driving supersaturation production. We agree with both reviewers that our explanation is incomplete, and derives from a too-literal interpretation of our Equation (1). We've re-written the discussion (which occurs several times, as indicated in the next two comments) to emphasize the role of water vapor availability/reduction in controlling the maximum supersaturation.
- **P9/L10**: See previous comment
- **P10/L7,15**: See previous comment
- **P12/L15**: Re-worked the discussion on the limitations of our methodology in the consolidated Sections 2 / 3.
- **Figures 5-8**: We note that the discussion which includes Figure 5-8 still draws samples from the set of uniform distributions described in Table 2, which were constructed using the observed ranges of aerosol size distribution parameters sampled from MARC. However, the first sampling study presented in the manuscript assumes these distributions to be independent, which is where the potential for non-physical combinations arises. We've tried to re-balance the discussions of our results more towards the aerosol size distributions sampled from MARC.

Reviewer #2

Major Comments

1. **Structure and Length of the manuscript**

   We have embraced all three reviewers' comments about the structure and length of manuscript and have undertaken substantial revisions and re-writing to address them. Specifically:

   a) The introduction has been nearly entirely re-written. We've removed references to studies of processes irrelevant to the results we present in this manuscript.

   b) We agree that the discussion of the small role of nucleation mode aerosol in activation dynamics is redundant. Section 2 has been consolidated and merged with Section 3. However, we have tried to retain some discussion and analysis of the iterative calculations, since we believe this procedure is more widely useful. Please refer to the comments at the beginning of this document for more information.

   c) Similar to the previous comment, we emphasize that our attempt to consolidate Sections 2 and 3 addresses this issue pertaining to reporting results which are not new.

2. **Comparison to other activation schemes**

   We agree with the reviewer that there is an inherent "unfairness" in evaluating the ARG and MBN schemes against our own parcel model and our sets of input parameters, and as the reviewer notes, we allude to this in the Conclusion. In the revised manuscript we bring up this point of discussion earlier. However, we do wish to emphasize that regardless of how a given scheme has been developed, to predict online CDNC in a global model, it must be coupled to some representation of an aerosol size distribution which may fall far outside the parcel model evaluations used to initially fit the scheme. As a result, it is critical to document the performance of these schemes in these extreme scenarios, which can and do arise in numerical models. We have attempted to clarify this discussion in the manuscript.

3. **Features of the aerosol size distribution in MARC**

   Table 2 provides some perspective on the distribution of MOS hygroscopicity - in the model, it is restricted to vary between 10^{-10} and 0.507 (volume-weighted mixtures of OC and SO4). In practice, it takes a mean value of 0.27 ± 0.04 (1 standard deviation). We've clarified in the manuscript that the relative abundance of OC and SO4 dominates the small variation in κ_{MOS}. In MAM3, primary organic carbon is assumed to have a κ of 0.1, which would tend to increase this average value, although we note that the presence of SOA, BC, and dust - all of which have smaller κ than sulfate - would tend to reduce the average value away from that of pure sulfate. Additional analysis using a variance-based decomposition and the derived metamodels (following Rothenberg and Wang (2016)) suggests that the hygroscopicity of MOS plays a very small role in influencing droplet nucleation given our particular aerosol size distribution, and instead the size and abundance of sulfate is more important.

4. **Previous work (Rothenberg and Wang, 2016)**

   We agree with the reviewer that deferring the reader to our previous study helps to streamline the present one, and have undertaken to do so while revising the manuscript. The new content here - which we emphasize in the revised manuscript - is the application to a more complex aerosol size distribution, and the training of a metamodel for use in predicting online cloud droplet number concentration in a global model which uses that aerosol size distribution.

5. **Role of gCCNs**

   We've expanded our discussion of Figure 10 to put this result in the context of previous work on role of gCCN, especially in clean environments.

6. **Applicability of the emulator**

   We wish to emphasize that the emulators were in fact trained to be able to cover extremely clean conditions (see Table 2, which indicates the ranges of size distribution parameters included in the training). Figures 5 and 7 further illustrate that the emulators perform at least as well as the ARG and MBN schemes in extremely clean conditions, too. We have focused the discussion in the revised manuscript more towards the activation of aerosol size distributions sampled from MARC directly to clarify these points. We have also included a discussion of the computational performance of the schemes.

Minor Comments

1. **P1/L3-4**: We agree on this detail, and have added this caveat.
2. **P2/L17** and **P18/L35**: Changed "processes" to "effects"
3. **P6/L18**: The minimum is set to 0.2 m/s and the maximum to 10 m/s; we've tried to make this clearer.
4. **P8/L30**: This point was also raised by Reviewer #1. We've re-worded this discussion to de-emphasize the role of latent heat release and instead focus on water vapor reduction, which is a more important influence on supersaturation development.
5. **P10/L18**: Re-phrased as just "cloud droplets"
6. **P10/L19,27**: We've adopted the the phrasing recommended by the reviewer.
7. **P12/L25,26**: We've re-written this to express our intended point, which was that in Rothenberg and Wang (2016), predicting $S_{\max}$ and then diagnosing N_{act} tended to be more accurate than predicting N_{act} directly as an emulated response.
8. **P17/L29**: Rephrased with more specifics on how activation is part of a fundamental relationship between aerosol and CDNC, and how this influences the indirect effect.
9. **P18/L27**: Clarified that Gantt et al. (2014) used different activation schemes to simulate cloud radiative effect and in the global average, these effects differed by 0.9 W/m^{-2} depending on the scheme used.
10. **P19/L1**: Rephrased sentence to avoid this vagueness.
11. **P19/L5**: We agree that this point should be made much earlier in the manuscript, and have included it towards the end of our revised Introduction as a motivation for further development of activation schemes.
12. **Figure 1**: Added a gap on the y-axis as recommended, and revised figure aesthetics.
13. **Figure 3**: We've adopted this recommendation and replaced the figure with a simple description in our revised Sections 2/3.
14. **Figure 4**: Labels are now defined in the caption.
15. **Figure 5**: Removed "one-one plot comparing" from caption.

Technical Comments

1. **P2/L2**: Included this grammatical change.
2. **P2/L18**: Corrected
3. **P2/L19**: Sentence does not appear in revised Introduction.
4. **P3/L10**: Fixed in BibTeX file with references.
5. **P5/L6**: Corrected
6. **P5/L17**: Corrected
7. **P6/L33**: Added definition
8. **P10/L10**: Equations are removed in revised Sections 2/3 in lieu of a reference to Rothenberg and Wang (2016) and standard texts
9. **P12/L21-22**: Corrected. "Activate" was missing
10. **P15/L34**: Corrected
11. **P17/L23**: Rephrased to avoid awkwardness
12. **References**: We use the provided BibTeX bibliography format and will consult with the editor on an appropriate course of action; Updated the Morales Betancourt and Nenes (2014) reference.

Reviewer #3

General Comments

1. **Computational Expense**

   We've included an assessment of the computational cost of running the CESM/MARC with the different activation schemes compared in this work, and our new emulators.

2. **New developments in this study**

   In line with the previous general comment, we indicate in the manuscript that the emulators derived here are implemented in the CESM/MARC to calculate online CDNC. We further clarify that the work necessary to accomplish this implementation (documented in the manuscript) is major advance beyond Rothenberg and Wang (2016), which only attempted to apply the PCM to emulate a parcel model using idealized, single-mode aerosol distributions.

3. **Length of manuscript**

   Following the comments made at the beginning of this document, we have substantially revised the manuscript by re-writing the introduction, removing material redundant to Rothenberg and Wang (2016), and consolidating Sections 2 and 3. We defer including a table of GCMs and their activation schemes, instead referring the reader to Table 3 of Ghan et al. (2011). In lieu of a pros/cons table for each scheme, we have simply truncated the discussion of each, referring the reader again to Ghan et al. (2011) and other works for more information.

4. **Exclusion of aerosol modes**

   In revising our discussion of the iterative calculations, we have removed the example figure which was the source of aerosol mode confusion here. To the broader point about justifying exclusion of some of the aerosol modes and parameters, we disagree here. The OC and BC modes are excluded by assumption (they are hydrophobic with $\kappa \approx 0$). Reviewers #1 and #2 strongly emphasize that nucleation mode aerosol do not contribute significantly to activation, which we agree with. No other modes are immediately excluded. The basis for excluding the Aitken and larger dust and sea salt modes follows the results of our iterative calculations. We've added some discussion on this point to the consolidated Sections 2 and 3, but for brief reference here: in general, the largest dust and sea salt modes exceedingly rarely have number concentrations greater than 1 per cm^3, which explains why they appear as a "dominant" mode in no case of our iterative calculations. The Aitken mode in MARC is generally small (see Table 1), which limits its influence on activation, although the reviewer's comments about the nucleation (or Aitken) mode particles being large enough in number concentration to influence $S_{\max}$ by depleting available water vapor is still relevant. Still, we believe that the results of the iterative calculations themselves provide a defensible basis for neglecting the MARC Aitken mode in the ultimate emulation parameter set.

5. **MBS hygroscopicity**

   In MARC, we assume MBS is constructed as a black carbon core fully covered by a sulfate shell. Therefore, the surface of such particles is assumed to be sulfate. In MARC, MBS forms from aging of external black carbon and continually grows from sulfate condensation and coagulation. Based on model results, the core-shell mass ratio is normally sufficiently small to support the assumption that the particle takes a hygroscopicity value comparable to that of sulfate.

6. **Sensitivity of emulator to training parameter set**

   We emphasize that our training dataset does not randomly sample from the distributions in Table 2; the probabilistic collocation method provides a particular algorithm for choosing the sample parameter sets, which are far more concentrated in the "center" of the high-dimensional set of input parameter distributions (that is, near the mean of each individual parameter distribution). The over-sampling of training parameter sets we choose is a compromise to include more of the very-high and very-low parameter values in the training dataset.

   The resulting emulator, though, should not be very sensitive to the exact choice of parameter set ranges. Following the recommendation of Rothenberg and Wang (2016), the final emulator is constructing using a least squares fit of the training parameters and the evaluated parcel model responses using a particular polynomial basis. However, the key ingredient here is the set of parcel model responses computed from the input parameter sets, which will not change unless the parameter space is dramatically altered.

   We do note, as the reviewer mentions, that some GCMs include a minimum threshold CDNC value as a tuning parameter; one reason to use activation schemes is to reduce the bias towards too-low CDNC in remote maritime regions which such a threshold aims to correct.

Minor Comments

1. **P2/L14-18**: This is removed in the revised Introduction.

2. **P2/L19**: We agree in principle, but also note that the representation of sub-grid scale processes in a GCM grid box also includes a distribution of updraft speeds, and merely an average aerosol size distribution (for instance, a grid box straddling a coastal area could include a large city and open water, and have vastly different aerosol populations in either side of the grid box depending on whether or not the flow is on/offshore). Robustly assessing activation in such a diversity of cases would require something akin to the multi-scale modeling frameworks which embed a cloud-resolving model in each GCM grid box, which we briefly mention in the manuscript.
3. **P4/L33**: Unfortunately, there is not yet a reference for the implementation of MARC in CAM5; our two references refer to the CAM3.5 implementation. We have revised the phrasing "extends".
4. **P5/L23-25,28-30**: MARC is just the aerosol model. We use the default CESM cloud microphysics.
5. **P5/L32-33**: We refer the reviewer to West et al. (2014), which includes a comprehensive assessment of the role of sub-grid scale vertical velocity on activation and cloud radiative effects, and note this in the manuscript.
6. **P6/L11**: Added emissions citations
7. **P6/L33**: Added definition
8. **P7/L1-7**: Deleted as part of the consolidated Sections 2 and 3.
9. **P7/L18-19**: We agree, but emphasize that this is an assumption and limitation in MARC - that MARC does not include a detailed representation of organic aerosol.
10. **P7/L21-22**: The NUC mode does not have a fixed size, but takes the range indicated from Table 2, which is restricted to be quite small. When larger sulfate particles form, mass and number is shifted to the larger modes, so the NUC mode can't contain CCN-relevant (by size) particles.
11. **P8/L26-30**: This discussion was simplified in the revised manuscript, and these statistics aren't discussed in the same way.
12. **P8/L31-32**: Added a note that the parameter sets were sampled from instantaneous MARC output between 70S-70N and below 500mb.
13. **P9/L11-13**: This is an interesting point, but we do not consider changes in parcel buoyancy in our parcel model simulations, which assume an adiabatic ascent.
14. **P12/L13-15**: We rephrased this entire discussion in response to another reviewer's comments, and this particular point is no longer emphasized.
15. **P12/L25**: Same as previous comment.
16. **P13/L19**: Changed sentence to read, "*Both the ARG and MBN schemes include some parameters fit to parcel model simulations conceptually similar to the one emulated here.*"
17. **P14/L8-13**: We've revised the discussion to focus more on the parameter sets sampled from online MARC simulations.
18. **P15/L32-33**: We refer to Table 2, which includes (in parentheses on the righthand columns) to percentile at which the lower/upper bounds chosen to train the model occur in the distribution of those parameters as sampled from MARC. The model does predict these very small values in some cases, although they are not physically significant.

19. **Figure5-8**: Added units to figure caption

20. **Table 2**: It's correct that κ_{MOS} can not exceed that of sulfate (0.507), but we train the model with a slightly larger range to better resolve that upper-most limit case. However, we note that the mean value of κ_{MOS} is 0.27 with a standard deviation of 0.04, so our range captures nearly the entire variability in its value.

References

Carslaw, K. S., Lee, L. a, Reddington, C. L., Pringle, K. J., Rap, a, Forster, P. M., Mann, G. W., Spracklen, D. V., Woodhouse, M. T., Regayre, L. a and Pierce, J. R.: Large contribution of natural aerosols to uncertainty in indirect forcing., Nature, 503(7474), 67–71, doi:10.1038/nature12674, 2013.

Gantt, B., He, J., Zhang, X., Zhang, Y. and Nenes, A.: Incorporation of advanced aerosol activation treatments into CESM/CAM5: Model evaluation and impacts on aerosol indirect effects, Atmospheric Chemistry and Physics, 14(14), 7485–7497, doi:10.5194/acp-14-7485-2014, 2014.

Ghan, S. J., Abdul-Razzak, H., Nenes, A., Ming, Y., Liu, X., Ovchinnikov, M., Shipway, B., Meskhidze, N., Xu, J. and Shi, X.: Droplet nucleation: Physically-based parameterizations and comparative evaluation, Journal of Advances in Modeling Earth Systems, 3(10), M10001, doi:10.1029/2011MS00007 2011.

Morales Betancourt, R. and Nenes, A.: Droplet activation parameterization: the population-splitting concept revisited, Geoscientific Model Development, 7(5), 2345–2357, doi:10.5194/gmd-7-2345-2014, 2014.

Partridge, D. G., Vrugt, J. a., Tunved, P., Ekman, a. M. L., Gorea, D. and Sorooshian, a.: Inverse modeling of cloud-aerosol interactions – Part 1: Detailed response surface analysis, Atmospheric Chemistry and Physics, 11(14), 7269–7287, doi:10.5194/acp-11-7269-2011, 2011.

Rothenberg, D. and Wang, C.: Metamodeling of Droplet Activation for Global Climate Models, Journal of the Atmospheric Sciences, 73(3), 1255–1272, doi:10.1175/JAS-D-15-0223.1, 2016.

West, R. E. L., Stier, P., Jones, A., Johnson, C. E., Mann, G. W., Bellouin, N., Partridge, D. G. and Kipling, Z.: The importance of vertical velocity variability for estimates of the indirect aerosol effects, Atmospheric Chemistry and Physics, 14(12), 6369–6393, doi:10.5194/acp-14-6369-2014, 2014.

An aerosol activation metamodel of v1.2.0 of the pyrcel cloud parcel model: Development and offline assessment for use in an aerosol-climate model

Daniel Rothenberg[1] and Chien Wang[1]

[1]Department of Earth, Atmospheric, and Planetary Sciences, Massachusetts Institute of Technology, Cambridge, MA, USA

Correspondence to: Daniel Rothenberg (darothen@mit.edu)

Abstract. ~~In order to simulate an aerosol indirect effect, most global aerosol-climate models utilize an activation scheme to physically relate the ambient aerosol burden to the droplet number nucleated in newly-formed clouds. While successful in this role, activation schemes are becoming frequently called upon to handle chemically-diverse aerosol populations of ever-increasing complexity. As a result, there is a need to evaluate the performance of existing schemes when interfacing with these complex aerosol populations and to consider ways to incorporate additional processes within them.~~

We describe an emulator of a detailed cloud parcel model which ~~can be used to assess aerosol activation, and compare it with two activation parameterizations used in global aerosol models~~has been trained to assess droplet nucleation from a complex, multi-modal aerosol size distribution simulated by a global aerosol-climate model. The emulator is constructed using a sensitivity analysis approach (polynomial chaos expansion) which reproduces the behavior of the ~~parent~~ targeted parcel model across the full range of aerosol properties ~~simulated by an aerosol-climate model. Using offline, iterative calculations with aerosol fields from the Community Earth System Model/Model of Aerosols for Research of Climate (CESM/MARC), we identify subsets of aerosol parameters to which diagnosed aerosol activation is most sensitive, and use these to train metamodels including and excluding the influence of giant CCN for coupling with the model~~and meteorology simulated by the parent climate model. An iterative technique using aerosol fields sampled from a global model is used to identify the critical aerosol size distribution parameters necessary for accurately predicting activation. Across the large parameter space used to train them, the ~~metamodels~~ emulators estimate droplet number concentration (CDNC) with a mean relative error of 9.2% for aerosol populations without giant ~~CCN~~cloud condensation nuclei (CCN), and 6.9% when including them. ~~Using offline activation calculations with CESM/MARC~~ Versus a parcel model driven by those same aerosol fields, the best-performing ~~metamodel~~ emulator has a mean relative error of 4.6%, which is comparable with ~~the two widely-used activation schemes considered~~ two commonly-used activation schemes also evaluated here (which have mean relative errors of 2.9% and 6.7%, respectively). We identify the potential for regional biases ~~to arise when estimating droplet number using different activation schemes~~in modeled CDNC, particularly in oceanic regimes, where our best-performing emulator tends to over-predict by 7%, whereas the reference activation schemes range in mean relative error from -3% to 7%. ~~In these offline calculations, the metamodels~~ The emulators which include the effects of giant CCN are more accurate in continental regimes (mean relative error of 0.3%), but strongly over-estimate ~~droplet number~~ CDNC in oceanic regimes by up to 22%, particularly in the Southern Ocean. The biases in ~~cloud~~

droplet number CDNC resulting from the subjective choice of activation scheme could potentially influence the magnitude of the indirect effect diagnosed from the model incorporating it.

1 Introduction

Ambient aerosol Aerosol play a critical role in the climate system by interacting with radiation through several different mechanisms. Depending on its their composition, aerosol particles can directly scatter or absorb incoming solar radiation, leading to a direct radiative effect and rapid changes in the energy budgets of the surface and atmosphere. Additionally, aerosol particles mediate the production of clouds by providing surface area on which water vapor may condense to form droplets. Through this second pathway, changes in the aerosol population perturb the radiative properties of clouds by altering their microstructure and lifecycle, thereby impacting the planetary radiative budget. Despite decades of focused research by the scientific community, the radiative forcing produced through this second pathway, known as aerosol-cloud interactions, remains one of the largest uncertainties in understanding contemporary and future climate change on both regional and global scales (Boucher et al., 2013).

Contemporary To include this second pathway, contemporary Earth System Models are a valuable tool for assessing this uncertainty. Compared to their predecessors, these models incorporate aerosol microphysics schemes which represent the global variation in particle size distributions and aerosol composition. These aerosol size distributions can then be used to predict cloud droplet number concentrationsconcentration (CDNC) by evaluating the nucleation of droplets (aerosol activation) from their simulated aerosol fields. As a result, changes in the aerosol size distribution due to anthropogenic emissions can impact cloud optical properties and produce an these models can resolve aerosol-climate indirect effectindirect effects which arise when anthropogenic aerosol emissions influence cloud microphysical and optical properties through impacting the CDNC burden. The interactions between aerosol particles, water vapor, and cloud droplets are often described using the conceptual model of a possibly-entraining, adiabatic cloud parcel (e.g. Feingold and Heymsfield, 1992; Nenes et al., 2001; Ervens et al., 2005; Topping et al., 2013). This parcel model framework provides a convenient means for both direct numerical and laboratory simulation of aerosol-cloud interactions, and has been used to establish the physical basis through which change sin the available aerosol perturb cloud radiative processes (Feingold et al., 2001).

However, it is not practical to directly include parcel model these calculations in global modelsdue to their coarse grid scales. Adiabatic , because of their computational complexity and because parcel theory describes a process which occurs on a spatial scale of tens of meters, over the course of a few seconds—occurring on spatial and temporal scales much finer than those resolved in many global model simulationsatmosphere models. Some efforts have sought to incorporate fine-scale information about aerosol-cloud interactions by embedding higher-resolution models within each grid cell of a global model (for example, the "multi-scale modeling framework" of Wang et al., 2011). However, while this approach has improved the representation of cloud processes in global models, it still does not resolve the scales of motion , but these are also too coarse to resolve the fine scale motions associated with parcel theory. To bridge this gap in spatial scalesresolve these issues, global

models employ ~~activation parameterizations which predict cloud droplet number concentrations using information about the subgrid-scale variability in meteorology and aerosol size distribution~~aerosol activation parameterizations.

~~Twomey (1959) first developed a scheme for placing an upper bound on this number of droplets derived from geometrical arguments applied to parcel theory. In subsequent decades, these arguments were used in conjunction with aircraft measurements to broadly characterize typical cloud droplet numbers in different regimes. For instance, Boucher and Lohmann (1995) developed power-law relationships between droplet number and sulfate mass concentration for separate continental and maritime regimes; similarly, Jones et al. (2001) developed a global parameterization for droplet number based on total aerosol number concentration using a survival function. While appropriate for earlier climate models which did not seek to resolve the complexity of the ambient aerosol, contemporary coupled aerosol-climate and aerosol-cloud-resolving models include more details about aerosol properties which can be used to predict cloud droplet number through explicit activation calculations. Broadly speaking, efforts to improve these activation calculations have proceeded down two avenues: caching of pre-computed,~~ A comprehensive review of the development of these parameterizations is provided by Ghan et al. (2011). In broad terms, there are two families of such schemes: look-up tables based on detailed parcel model calculations ~~; and extensions to Twomey's geometrical arguments using~~ (e.g. Saleeby and Cotton, 2004; Ward et al., 2010), and physically-based ~~approximations.~~

~~The simplest technique applied to parameterizing aerosol activation is to pre-compute, using a detailed parcel model , a set of aerosol and meteorological conditions sampled over some pre-determined parameter space (Saleeby and Cotton, 2004; Ward et al., 2010). These samples can then be used to construct a~~ parameterizations (e.g. Twomey, 1959; Ghan et al., 1993; Abdul-Razzak and Ghan, 2000; Co Physically-based approaches often rely on empirical fits or tuning derived from parcel model calculations, but are preferable for inclusion in regional or global climate models, because they are usually applicable to an arbitrary description (modal or sectional) of the aerosol size distribution. New look-up ~~table, using some form of interpolation to compute activation results for points within the domain of the initial parameter space. However, changing or increasing the number of parameters—such as including additional aerosol modes or a composition dimension—in the~~ tables must be computed whenever additional aerosol parameters are introduced; this is a problem because a look-up table~~rapidly increases its computational cost, since it is costly to both store and access the required information in memory during run-time.~~

~~Alternatively, one can extend Twomey's analytical approach to bounding the maximum supersaturation achieved in the constant-speed, adiabatic ascent of a parcel (e.g. Cohard et al., 1998; Cohard and Pinty, 2000). Several techniques have been employed to account for the sensitivity of the maximum supersaturation achieved by such a parcel to variations in the initial dry aerosol particle size distribution (Khvorostyanov and Curry, 2006; Shipway and Abel, 2010; Shipway, 2015). These techniques yield closed-form expressions which relate the parameters describing the initial aerosol size distribution and updraft speed to the supersaturation maximum, and can be used to predict droplet number concentrations for a given scenario.~~

~~Such studies have led to a number of explicit activation schemes, each applying a different computational and analytical approach but fundamentally relying on the same set of physical approximations (see Ghan et al., 2011, for a more complete review). Some of these schemes have been extended~~ 's size grows exponentially as the number of parameters included increases. But look-up tables offer some advantages, including computational efficiency and the ability to account for ~~additional physical or chemical processes which can influence activation, such as the presence of organic surfactants on the surface of droplets~~

which tends to reduce surface tension (Abdul-Razzak and Ghan, 2004), or to account for entrainment in the ascending parcel (Barahona and Nenes, 2007). These schemes generally rely on iterative calculations to settle on an estimate of how many aerosol particles activate into cloud droplets (e.g. Shipway and Abel, 2010; Nenes and Seinfeld, 2003; Ming et al., 2006), although some employ pseudo-analytical solutions to avoid this process (Abdul-Razzak et al., 1998).

Since they offer generalized formulations independent of the representation of the aerosol particle size distribution provided to them, physically-based schemes have been the preferred tool for coupling with global aerosol-climate models. But, they are not without their shortcomings. Simplifying assumptions used to construct physically-based schemes, such as particles' equilibrium growth in response to changes in the ambient relative humidity, neglect biases in estimating CDNC, such as kinetic limitations on growth and also lead to an underestimate in cloud droplet number in both polluted conditions and ones with weak updraft speeds (Nenes et al., 2001). Some schemes tend to under-estimate the number of droplets nucleated droplet growth (Nenes et al., 2001), the co-condensation of organic vapors (Topping et al., 2013), and competition for water vapor uptake in the presence of multiple , competing aerosol modes , owing to their representation of water vapor uptake by particles (Simpson et al., 2014). Although Gantt et al. (2014) showed that using a variety of activation schemes in a modern aerosol-climate modelwith a complex aerosol particle size and composition distribution can lead to a global increase of estimated cloud droplet number by 155%, many evaluations of activation scheme performance have focused on the same set of relatively simple aerosol particle size distributions. For instance, Abdul-Razzak (2002) used the Whitby (1978) aerosol particle size distributions but with only two aerosol composition scenarios, varying the insoluble mass fraction in the coarse aerosol modebetween either 0% or 90%. Nenes and Seinfeld (2003) and Fountoukis and Nenes (2005) used the same aerosol particle size distributions, but assumed just one additional aerosol composition scenario, exploring the impact of aerosol which are composed of 20% (by mass) of an organic which displays surface-active behavior; Ming et al. (2006) employed an identical set of evaluation simulations. Shipway and Abel (2010) restricted the analysis of their scheme's performance with multi-modal aerosol particle size distributions to an idealized bi-modal distribution with non-varying, homogeneous particle composition. Ghan et al. (2011) summarized the performance of all of these simulations with the same set of tri-modal aerosol particle size distributions, but extended their analysis to evaluate droplet number simulated by two schemes (Abdul-Razzak and Ghan, 2000; Fountoukis employed in a global model. Meskhidze (2005) used in situ data collected from two different aircraft observation campaigns to evaluate the sectional formulations of the Nenes and Seinfeld (2003) and Fountoukis and Nenes (2005) schemes; these evaluations were extended by Fountoukis et al. (2007), which analyzed the modal formulations of the same schemes, and Morales et al. (2011) which showed that accounting for entrainment reduced the over-prediction of droplet number in stratiform clouds by the activation schemes.aerosol modes (Simpson et al., 2014).

However, look-up table approaches do not necessarily solve these shortcomings. Detailed parcel models can more easily accommodate additional physics and chemistry which influences aerosol activation, but it would not be practical to incorporate this information into a look-up table. However, in previous work, Rothenberg and Wang (2016) Rothenberg and Wang (2016) previously used statistical emulation to conduct a sensitivity analysis of a detailed parcel model, focusing on a single, lognormal aerosol mode. Other studies have also used emulation approaches to study response surfaces of both cloud parcel models (Partridge et al., 2011) and global models (Carslaw et al., 2013), but Rothenberg and Wang further developed a framework for producing an emulator of

a detailed parcel model, which could be used to extend the benefits of using their emulators as an activation parameterization, which they compared to a high-dimensional extension of traditional look-up tablesto high-dimensional parameter spaces. In their example, which focused on the activation of a single lognormal aerosol mode, the meta-models produced by such a framework had lower error statistics on average than existing activation schemes when compared to a benchmark parcel model. Compared to two other physically-based schemes, the emulator-activation parameterizations tended to predict CDNC more accurately versus a reference parcel model, particularly in regimes with weak updraft speeds and high aerosol number concentration, where the traditional parameterizations performed the most poorly.

In this present work, we extend the methodology developed in Rothenberg and Wang (2016) to develop an emulator suitable for inclusion in a modern, coupled this approach to develop a set of metamodels trained for the aerosol and meteorology parameter space simulated by a global aerosol-climate model. Furthermore, we assess the performance of the emulator against existing activation schemes across a large input parameter space and a subset reproducing the tendencies of the aerosol-climate model. By reproducing the original, detailed parcel model on which it is trained, such an emulator could reduce biases in estimates of cloud droplet number concentration in cloud regimes characterized by either high pollution or relatively weak forcing and ascent. This could in turn lead to improved estimates of the aerosol indirect effect from global models. The resulting metamodels can thus be directly used as activation parameterizations inside a global climate to predict online CDNC, given information about the aerosol size distributions and sub-grid scale meteorology in each model grid-box. To refine the parameter space used for emulation, we present an analysis of how the size distribution parameters of each aerosol mode in our model contribute to activation dynamics and droplet nucleation. We then evaluate the performance of our emulator-parameterizations versus two physically-based schemes which are used in the vast majority of contemporary global models (see Table 3 of Ghan et al., 2011), and assess the impact of including each of these schemes on the computational expense of our global model.

This manuscript is organized to reflect the exploratory process used to develop the activation emulator presented here, with the hope that clearly delineating the steps involved will encourage other groups to pursue similar lines of work. **??** provides background on the parent aerosol-climate model for which our activation emulator was derived. Section 2.1 details the construction of the emulators and the tools used to produce them. Two different evaluations of the emulators are presented in Section 3. Finally, in Sect. 4 we motivate future projects using these emulators and, more broadly, this approach to building parameterizations.

2 Activation Parameter SpaceEmulation of aerosol activation

The parent aerosol-climate model for which we

2.1 Parent aerosol-climate model

We seek to derive a aerosol activation emulator is aerosol activation emulators for the MultiMode, two-Moment, Mixing-state resolving Model of Aerosols for Research of Climate (MARC; version 1.0.1 here) (Kim et al., 2008, 2014). MARC extends builds on the NCAR Community Earth System Model (CESM; version 1.2.2 here), which is a fully-coupled global climate model with sub-components for simulating climate processes in the land, ocean, atmosphere, and sea ice domains. In

particular, MARC replaces the default modal aerosol treatment (Liu et al., 2012) in the atmosphere component of the CESM, the Community Atmosphere Model ~~(CAM5; version 5.3 here)~~(CAM5; version 5.3 here Neale et al., 2012), with a scheme which simultaneously resolves both an external mixture of different aerosol species and internal mixtures between others (Wilson et al., 2001).

~~In this sense, MARC refers to a configuration of the CESM with the CAM5 atmosphere component and the alternative aerosol formulation.~~

~~The aerosol population within MARCis comprised of a~~ Table 1 summarizes the aerosol modes predicted by MARC, which includes tri-modal sulfate ~~distribution~~ (nucleation ["NUC"], ~~aitken~~ Aitken ["AIT"], and accumulation ["ACC"]~~modes~~), discrete modes for pure black carbon ("BC") and a generic organic carbon species ("OC"), and two "mixed" modes, one of each for mixed sulfate-black-carbon ("MBS") and sulfate-organic-carbon particles ("MOS"). ~~The ratio of the masses within each mixed species evolves over time, changing the optical and chemical properties of those particles.~~ For each of these seven modes, MARC predicts total particle mass (M) and number concentrations (N) for a corresponding lognormal size distribution with a prescribed width (geometric standard deviation; σ_g), as well as the total mass of carbon in each of the MOS and MBS modes. Additionally, ~~both~~ sea salt ("~~SSLTn~~SSLTn") and dust ("~~DSTn~~DSTn") particle size distributions are each described within MARC ~~by~~ using a 4-bin, single-moment scheme with fixed particle sizes ~~. For these single moment modes, MARC predicts a total number concentration for each bin and then diagnoses a total mass in order to simulate a lognormal mode with prescribed geometric mean radius (which is narrower for super-micron dust and sea-salt)~~and an assumed σ_g. Each mode has a prescribed particle hygroscopicity follow κ-Köhler theory (Petters and Kreidenweis, 2007) except for the MOS mode, which has a composition-dependent κ computed assuming that the carbon and sulfate in the particle ~~forms~~ form a simple internal mixture. Unlike the MOS mode, the MBS mode assumes a core-shell structure with sulfate coating a black carbon nucleus, and has a fixed hygroscopicity corresponding to that of sulfate, $\kappa = 0.507$. The sea salt modes are assumed to be comprised of NaCl with $\kappa = 1.16$, and the dust modes are assumed to be a mixture of minerals with a hygroscopicity of $\kappa = 0.14$ (Scanza et al., 2014). The ~~organic and black carbon~~ OC and BC modes are assumed to be non-hygroscopic and not significant players in aerosol activation.

~~These assumptions about the aerosol size distribution simulated by MARC are summarized in Table 1.~~

The aerosol size distributions predicted by MARC interact with both radiation and cloud microphysics. ~~With respect to the latter, MARC adopts the~~ MARC uses a two-moment, stratiform cloud microphysics scheme ~~found by default in CAM5 (Morrison et al., 2008) which provides~~ (Morrison et al., 2008) which includes an explicit source of cloud droplet formation via aerosol activation~~from aerosol. This interaction~~ . This is facilitated by means of a physical parameterization which takes as input both the physical and chemical properties of the ambient aerosol as well as limited information about meteorology ~~—in particular~~such as, the distribution of subgrid-scale vertical velocities. In ~~MARC~~CAM5 (as used by MARC), a single ~~subgrid-scale~~ characteristic updraft velocity (V) diagnosed from the grid cell turbulent kinetic energy (TKE) provided by the moist turbulence scheme (Park and Bretherton, 2009) and assumed to be isotropic is used to estimate droplet nucleation following Ghan et al. (1997) and Lohmann et al. (1999), such that

$$V = \overline{V} + \sqrt{\frac{2}{3}\mathrm{TKE}}$$

where $\overline{V}$ is the large-scale resolved updraft velocity. Furthermore, we limit ~~$V > 0.2\,\mathrm{m\,s^{-1}}$~~ $0.2\,\mathrm{m\,s^{-1}} < V < 10\,\mathrm{m\,s^{-1}}$ because the processes driving turbulence are not represented well in MARC, particularly those driven by cloud-top radiative cooling above the planetary boundary layer (Ghan et al., 1997). Morales and Nenes (2010) and West et al. (2014) have explored how using different characteristic updraft velocities to represent subgrid-scale variability can influence simulated aerosol-cloud interactions; in particular, West et al. (2014) showed that using a similar TKE-based parameterization produced more realistic spatial and temporal variability in V, but tends to produce an unrealistically high frequency of its minimum-permissible value. We further assume that activation ~~only~~ occurs in non-entraining, adiabatic updrafts which carry air up and into the base of stratiform clouds.

2.2 ~~MARC~~ Aerosol ~~and Meteorology Parameters~~activation parameter space

~~The set of size distribution parameters describing each aerosol mode in MARC and the number of meteorological factors influencing droplet nucleation in MARC is large, and each parameter can vary over several orders of magnitude across the globe in even a single timestep~~MARC requires 24 parameters to fully describe its 15-mode aerosol size distribution, although not all of these modes are important for aerosol activation. Activation calculations additionally require three meteorological parameters (temperature, pressure, and V). To assess this parameter space, we sample ~~instantaneous snapshots of the 3D~~ 70 snapshots of instantaneous aerosol and meteorology fields ~~from a MARC simulation run~~ produced by a simulation of MARC forced with present-day aerosol and precursor gas emissions ~~. In total, 70 timesteps were sampled covering the complete seasonal and diurnal cycle at each model grid cell.~~ (Kim et al., 2014), and with interactive dust (Albani et al., 2014) and sea salt (Mårtensson et al., 2003) emissions. Only grid-cells located below 500 mbar and between 70S and 70N were included in this assessment, since this is where liquid clouds and droplet nucleation are most prevalent in the model.

~~The variability in sub-grid scale vertical velocity as a function of continental versus maritime grid cells across all time samples in this output is summarized in Fig. 1. In both regimes, the mode updraft speed falls at the~~ As shown in Fig. 1, V tends to take the lower bound of $0.2\,\mathrm{m\,s^{-1}}$ ~~, and occurs about~~ nearly 50% of the time ~~. These velocities~~ in this sampling dataset and rarely exceed $1\,\mathrm{m\,s^{-1}}$ ~~- 10% and 1% of the time over land and ocean, respectively~~. On average, ~~land velocities are~~ in continental regimes V is slightly larger ($0.41\,\mathrm{m\,s^{-1}}$ vs $0.32\,\mathrm{m\,s^{-1}}$ in ocean regimes), but ~~have higher variance. The distribution of vertical velocities in both regimes~~ has a long~~positive tail,~~ , positive tail maxing out between $3\,\mathrm{m\,s^{-1}}$ to $4\,\mathrm{m\,s^{-1}}$ ~~and never approaching the artificial cap imposed by MARC~~. The upper bound on V is never reached in our model output sampling.

The ~~different particle size distributions in MARC are influenced by both different emissions sources and acted upon by different physical processes. This leads to a great deal of spatial heterogeneity in the~~ distributions of key aerosol size distribution parameters ~~. One aspect of this heterogeneity is depicted in **??**, which shows distributions of the total number concentration of four of the modes aggregated into latitude and height bins. In general, number concentration for each mode decreases with height, as expected since (with the exception of the pure sulfate modes) all the modes have strong sources near the surface in~~

the model. Natural aerosols (dust and sea salt) are generally much less abundant than anthropogenic ones. Furthermore, there are generally more aerosol by number in the Northern Hemisphere than in the Southern Hemisphere to the preponderance of anthropogenic emissions sources.

Many of the distributions featured in **??** have long tails extending towards very low number concentrations. These very low values can be problematic for activation parameterizations, especially those constructed from statistical methods or sampling, such as a lookup table, as they necessitate many saved interpolation points. However, aerosol activation produces at most one droplet per aerosol, so sensible lower bounds can be imposed to create a minimum threshold below which little activation is assumed to occur. Furthermore, are shown in Fig. 2. Because particle size is a critical factor size in assessing aerosol activation; larger particles have a much lower barrier to activation following Köhler theory (Seinfeld and Pandis, 2006). To simplify the assessment of how activation is influenced by the simulated aerosol size distributions in MARC, we diagnose , we show distributions of μ_g from the prognostic moments output by MARC, and study it in lieu of the total mass concentration (, the geometric mean radius, instead of M).

Although there is a great deal of variability in the number concentrations simulated by MARC, for all but the nucleation mode sulfate and coarse dust and sea salt modes, those values are most often drawn from a range of just a few . Many size distribution parameters can vary over several orders of magnitude . In general, the number burden in each mode approximately scales with the total aerosol burden. Put another way, the number concentrations in the main sulfate and carbonaceous modes tend to correlate strongly with one another, as does each mode 's corresponding mean size. In contrast, the number of sea salt particles tends to be much greater in the remote maritime environment where there are fewer particles overall (by number). The overall range of geometric mean mode particle sizes tends to be smaller than the range in number concentrations for each corresponding mode.

2.3 Reducing the Parameter Space

In total, MARC simulates 15 modes - seven double-moment and eight single-moment. As a result, we require 22 parameters to completely describe the aerosol sizedistribution. Two parameters are needed to close the description of its composition; the hygroscopicity and density of the MOS mode evolves in response to its relative mixture of carbon and sulfate, across the globe in even a single timestep. Values for N and μ_g in each mode tend to co-vary, though there is significant hetereogeneity in the overall aerosol mixing state (not shown here). For most modes, the parameter distributions have long tails where N and the MBS mode accrues sulfate mass through aging, which also impacts its particle density. Finally, the ambient temperature and pressure, as well as the vertical velocity of the updraft in which activation is occurring are meteorological parameters which can influence the droplet number nucleated. This yields a total activation parameter space with 27 independent dimensionsμ_g are both small. In these cases, few particles are likely to activate due to their small size, and would yield few cloud droplets even if they did. The number concentrations of DST and SSLT mode particles are typically very small compared to those in the ACC, MOS, and MBS modes. Aitken-mode particles in MARC are generally small but numerous, based on how the mode is defined in the model (Table 1). We note that on average, MOS-mode particles have an intermediate κ of 0.27 ± 0.04 (standard deviation) which varies with local sulfate abundance.

The emulation method used by Rothenberg and Wang (2016) is designed to work with an arbitrary ~~number of input parameters~~input parameter space. However, ~~in order to focus our analysis on those parameters most influential on predictions of droplet nucleation,~~ we restrict the ~~input~~ aerosol activation emulation parameter space by eliminating parameters which exert little or no influence on the activation process. ~~For instance, the pure carbonaceous modes (~~This reduces the number of parcel model simulations necessary to train emulators as well as their complexity. The OC and BC ~~) are hydrophobic and not sources of CCN, so we neglect them in the activation calculation. The nucleation mode sulfate typically has much fewer and much smaller particles than the Aitken mode and accumulation modes present in a grid cell. Furthermore~~modes are assumed to be hydrophobic and hence cannot serve as cloud condensation nuclei (CCN); NUC particles are typically too small to serve as CCN, although they could be present in large enough number to influence supersaturation and droplet nucleation. However, where nucleation mode particles are ~~abundant in number, the other sulfate modes generally are , too. Thus, we also assume that the nucleation mode is not a source of CCN, and exclude it from our activation calculations. Additionally, the mixed black-carbon-sulfate mode (MBS) is assumed to be composed of particles with a carbon core and sulfate shell; we further assume that the entire surface of these particles are coated, effectively rendering the MBS particle hygroscopicity to be equal to that of sulfate. These assumptions effectively reduce the number of parameters we must consider by seven, bringing the initial parameters to a set of 17 aerosol ones and 3 meteorological ones.~~ usually most abundant when larger sulfate particles (especially ACC) are also present in large concentrations and have a greater influence on activation dynamics. We neglect size distribution parameters from these modes to build our emulators.

2.3 ~~Iterative Activation Calculations~~

To further reduce ~~this number~~the emulation parameter space, we assess the relative importance of each individual aerosol mode and its influence on activation dynamics ~~. This helps to identify a subset of aerosol modes to use as predictors in our emulator, avoiding the need to include all 17 potential aerosol parameters. We accomplish this with~~ using an ensemble of iterative, single-mode activation calculations using a detailed reference parcel model (Rothenberg and Wang, 2016)~~, drawn from a sample of aerosol size distributions simulated by MARC. This strategy effectively employs a "greedy" algorithm to sort the set of available aerosol modes, ranking their influence on activation by their cumulative depression on the supersaturation maximum achieved for a given parcel ascent.~~

~~Given a set of~~ . For each of our n aerosol modes, ~~the iterative calculations provide a sorted order for the modes, indicating their relative contribution to activation dynamics. Specifically, for each n modes,~~ we pick a test mode and run a parcel model simulation to compute the ~~minimum~~ supersaturation maximum ($S_{\max}$) achieved in an updraft in which that mode is embedded. The mode which produces the minimum $S_{\max}$ is said to be the "dominant" mode, and we record its size distribution. We then remove that aerosol from the original set of n modes~~. At this point, we~~ , and re-visit each of the $n-1$ remaining modes, ~~and run parcel simulations in which the first "dominant " mode is present along with one additional mode. Again, we record the minimum $S_{\max}$ and remove the contributing mode from the original set, adding it to the set of dominant modes.~~ including now the first dominant mode along with each new test mode. The end result of $n-1$ iterations is a ~~complete~~ sorting of the modes ~~,~~ based on their contribution to reducing $S_{\max}$ in the parcel model simulations.

?? illustrates this iterative process for an example marine aerosol distribution following Whitby (1978). In this example, all particles are assumed to be pure sulfate. The vast majority of particles exist in the smaller, nucleation mode, but the coarse mode dominates the mass distribution. Only when inspecting the surface area distribution do all three modes even become apparent. With respect to activation, the number of aerosol particles is critically important, because droplets must form from individual particles. Thus, it would be reasonable to assume that the nucleation mode particles would "dominate" activation in this case - or that small changes in the burden of these particles could have large consequences on how many cloud droplets will form.

However, that doesn't happen. On the right-hand panel of ?? are plotted traces of the supersaturation achieved in a parcel with the indicated aerosol population, as a function of height above the parcel's initial altitude. In the first iteration, the parcel achieved minimum supersaturation maxima of 1.2%, 1.4%, and 1.3% when just the accumulation, coarse, and nucleation modes are present, respectively. These are much higher supersaturations than the Köhler-theory critical supersaturation for the geometric mean particle size in both the accumulation and coarse modes (0.3% and 0.1%, respectively), and a large fraction of the particles in those two modes activate. However, the number concentration of particles in those two modes is very small (60 and 3.1 particles cm^{-3}), and it takes time before the latent heat release due to condensation balances the cooling in the ascending parcels. Although the nucleation mode particles are much smaller and fewer of them activate, their number concentration is much higher ($340\,\mathrm{cm}^{-3}$) and the total liquid water condensed on them is similar through the ascending parcel's trajectory, hence the similar values for S_{max} in all three cases.

In the second iteration—with the accumulation mode omnipresent—the coarse and nucleation modes only reduce S_{max} to 0.96% and 1.08%, respectively. The final iteration, which includes all three modes, produces an S_{max} of 0.92% with an ordering of (accumulation, coarse, nucleation). These reductions in S_{max} are due to the higher total particle number concentration and surface area available for condensation which leads to a more rapid balancing between the parcel's adiabatic cooling and warming due to latent heat release.

We apply this algorithm to a sample set of 50,000 aerosol size distributions and meteorological distribution and meteorology parameters taken from our reference , present day MARC simulation. For each parameter set, we calculate the first four dominant modes, and record the supersaturation maxima produced by each successive combination. Using these supersaturation maxima, we diagnose the number of activated aerosol across the total aerosol population, including modes which are not present in the parcel model simulation at a given iteration. Additionally, for each parameter set we perform a reference parcel model calculation where all aerosol modes are included, for comparison with the iterative calculations.

Overall, the accumulation mode sulfate (ACC) Overall, ACC is the dominant mode in 96.5% of the sample cases. Infrequently, the mixed-sulfate-carbon modes and smallest dust mode MOS and small dust (DST1) are the dominant mode, accounting for all of the remaining cases. When ACC dominates the activation dynamics, either the mixed-modes (MBSand MOS) MBS/MOS or smallest sea salt mode (SSLT1) is the second-most dominant one (in 10.3%, 36.2%, and 52.8% of cases, respectively). In fact, this ordering is so common that in 85% of all the sample cases, three of ACC, MOS, MBS, or SSLT01 comprise the top three dominant modes.

Figure 3 illustrates the potential error in calculating both S_{max} and N_{act} (number concentration of activated particles or CDNC) for each iteration of the activation calculations relative to using the ~~full~~ complete MARC aerosol population, aggregated by ~~which mode was the first-most dominant one. In all cases, using~~ the first dominant mode. Using a subset of the modes ~~tends to over-predict the droplet number activation as a consequence of~~ leads to an over-prediction of N_{act} due to predicting a high value for S_{max}. This is consistent with the physics of the activation problem; the presence of more aerosol surface area on which condensation can occur tends to ~~produce a greater source of latent heat release to counter-balance adiabatic cooling~~ deplete water vapor in the ascending parcel more quickly, suppressing the development of a higher S_{max}. But as Fig. 3 shows, this over-prediction decreases rapidly as additional modes are included in the calculation. Part of this decrease is related to the fact that adding modes in each iteration captures a higher fraction of the total aerosol number; on average, the first dominant mode contains $70\% \pm 27\%$ of the total aerosol number, which increases to $80\% \pm 17\%$ and $89\% \pm 13\%$ after adding the second and third modes. Following this increase in fraction of the total aerosol number included by the dominant mode set in each iteration is a decrease in the absolute error in N_{act} relative to the full aerosol population, with an average of less than $1\,\mathrm{cm}^{-3}$ and max of $57\,\mathrm{cm}^{-3}$ by the third iteration. Although giant CCN particles are well-represented in MARC by dust and sea salt modes, they are typically too few in number to largely influence droplet nucleation except in rare cases where other modes are not abundant.

~~With respect to the goal of reducing the aerosol parameter space necessary for assessing aerosol activation, what's more important in these calculations than the frequently dominant modes, though, is the the absence of several modesaltogether. In particular, the Aitken mode sulfate is never one of the first three dominant modes; beyond the modes depicted in Fig. 3, the only other modes in that set are the larger dust and sea salt modes. But in nearly all the cases sampled here, those modes have number concentrations that decrease as the bin's particle size increases. Also, the smallest dust and sea salt bins tend not to feature very high number concentrations in the first place. Even though the larger bins contribute particles which will almost always activate, owing to their size and composition, the particles in them simply aren't numerous enough to impact the activation calculations~~Based on the sampling and iterative calculations presented in this section, we define the activation emulation parameter space as in Table 2. We consider the full range of potential values for V, but restrict further the emulation to include the most frequent "dominant" aerosol modes. Table 2 further defines ranges considered for each of the aerosol and meteorological parameters, and indicates the percentile of the sampling data at which the extreme values of each range occur. In all cases we include upper bounds above the 98th percentile of the sampling data. For the giant CCN modes (DST and SSLT), we restrict the lower ranges of N but at values where small changes in N could only have very small contributions to changes in N_{act}.

3 ~~Emulator Development~~

2.1 Emulator construction

~~We now seek to construct an emulator of a detailed adiabatic cloud parcel model capable of resolving aerosol activation within an ascending, constant-speed updraft.~~ The following sections briefly describe the chosen cloud parcel model and emulation

technique, polynomial chaos expansion. For more details on both techniques and their application, we refer the reader to Rothenberg and Wang (2016), which derives activation emulators for a simplified, single lognormal aerosol mode.

2.2 ~~Parcel Model~~

2.1.1 Parcel Model

Adiabatic cloud parcel models are a standard modeling tool for detailed assessments of aerosol activation and other studies focused on the composition of atmospheric particulates (Seinfeld and Pandis, 2006). In such a model, a constant-speed updraft drives adiabatic cooling in a closed, zero-dimensional air parcel within which are any number or configuration of aerosol particles. Initially prescribed a temperature, pressure, and water vapor content, the cooling parcel eventually develops a supersaturation with respect to water vapor. In a sufficiently supersaturated environment, water vapor condenses on particulate surfaces. ~~However,~~ This condensation releases latent heat ~~, which counter-balances the parcel's adiabatic cooling . This balance~~ and slows down the cooling of the parcel, but more importantly acts to sink water vapor mass. In terms of producing supersaturation, these counter-acting processes can be expressed

$$\frac{dS}{dt} = \alpha(T,P)V - \gamma(T,P)\frac{dw_c}{dt} \tag{1}$$

where V is the updraft speed, $\alpha(T,P) = (gM_wL/c_pRT^2) - (gM_a/RT)$ and $\gamma(T,P) = (PM_a/e_sM_w) + (M_wL^2/c_pRT^2)$ are functions weakly dependent on temperature and pressure (Leaitch et al., 1986), M_w and M_a are the molecular weights of water and air, L is the latent heat of vaporization of water, c_p is the specific heat of dry air at constant pressure, R is the universal gas constant, g is the acceleration due to gravity, e_s is the saturation vapor pressure, and w_c is the liquid cloud water mass mixing ratio (please refer to Appendix A of Rothenberg and Wang, 2016, for more details).

At some time t, the balance between heating due to latent heat release and cooling due to the parcel's adiabatic ascent will approximately balance such that $\frac{dS}{dt} = 0$ and a supersaturation maximum, $S_{\max}$, will occur. Thereafter, S generally decreases, relaxing to some value close to unity as condensation drives droplet growth, quenching the ambient water vapor surplus. Beyond this point, the aerosol bifurcates into two populations: ~~proto-cloud~~ new cloud droplets which will continue to grow due to condensation and eventually collision and coalescence, and interstitial haze particles which may have ~~become hydrated~~taken up some water according to their hygroscopic mass, but upon which further condensation is not thermodynamically favorable.

~~In order to compute these effects, we simulate an arbitrary number of initial dry particle size distributions following a lognormal assumption:~~

$$n_N(r) = \frac{dN}{d\ln r} = \frac{N_t}{\sqrt{2\pi}\ln\sigma_g}\exp\left[-\frac{ln^2 r/\mu_g}{2\ln^2\sigma_g}\right]$$

~~Each aerosol mode is thus defined uniquely by three parameters (N_t, μ_g, σ_g) corresponding to the total aerosol number concentration, the geometric mean particle radius, and the geometric standard deviation. The modes are each further discretized~~

into a Lagrangian grid of 200 size bins, equally spaced over the logarithm of the particle radius such that each bin represents a different number of particles. The particles are then hydrated to an equilibrium size with respect to the initial relative humidity in the model; condensation acts to grow this size in response to the thermodynamic evolution of the parcel.

Furthermore, each bin is assigned a fixed hygroscopicity following κ-Köhler theory (Petters and Kreidenweis, 2007). By tracking the dry particle size, a hygroscopicity, and the wet radius of each particle, aerosol activation can be directly assessed within the model.

2.2 Polynomial Chaos Expansion

2.1.1 Polynomial Chaos Expansion

We emulate the behavior of the detailed parcel model by applying the probabilistic collocation method (PCM; Tatang et al., 1997). PCM is a method of polynomial chaos expansion which seeks to construct a model response surface by mapping input parameters related to the initial conditions and behavior of a model to some response measured from the model. This process yields a computationally efficient yet accurate reproduction of the model.

The PCM is a non-intrusive technique which does not require modifications to an existing model in order to be applied. Instead, the PCM treats the original, full-complexity model as a black box and the chosen set of M M' input parameters as independent, random variables, $\mathbf{X} = X_1, \ldots, X_M$ $\mathbf{X} = X_1, \ldots, X_{M'}$, each with an associated probability density function. This PDF is used as a weighting function to derive a family of orthogonal polynomials which are used as the bases for the polynomial chaos expansion to be constructed, ϕ. Using a finite number of these bases and choosing some model response, R, we write the polynomial chaos expansion as

$$R \approx \sum_{j=0}^{P} \alpha_j \phi_j(\mathbf{X}) \tag{2}$$

Such an expression has $N_t = P + 1 = (M + p)!/(M!p!)$ $N_t = P + 1 = (M' + p)!/(M'!p!)$ total terms, since a given chaos expansion of order p will contain $p + 1$ basis terms for each input parameter and combinations thereof. The coefficients α_j are computed by evaluating the original model at a set of particular set of sample points, recording the response of the model, and solving a regression problem. Those sample points are generated by taking the roots of the orthogonal polynomials associated with each of the input parameters and their random variables.

In order to compute the polynomial chaos expansions, we use the Design Analysis Kit for Optimization and Terascale Applications (DAKOTA; Adams et al., 2014), version 6.1. This software automates the process of generating input parameter sets, sampling the full-complexity model to be emulated, and constructing the polynomial chaos expansion. Furthermore, it provides many useful statistical properties of the sample dataset and the chaos expansions themselves.

2.2 ~~Emulation of aerosol activation for MARC~~

2.1.1 Application to MARC aerosol

We ~~now apply the~~ extend the idealized calculations in Rothenberg and Wang (2016) by applying the parcel model and chaos expansion technique ~~in the previous sections~~ previously described to construct emulators of aerosol activation suitable for use in MARC. ~~Following the analysis in ??, we identify a reduced-dimensionality input parameter space which covers the diverse set of aerosol and meteorology scenarios in which activation occurs in MARC, summarized by Table 2. Following the iterative calculations, we restrict the aerosol modes included in the activation calculation to just the accumulation mode sulfate and both mixed sulfate-organic carbon and sulfate-black carbon particles, as well as the two smallest dust modes and the smallest sea salt mode. To assess the importance of these less-abundant, coarse particles, we derive two emulators~~Using the parameter set and value ranges summarized in Table 2, we consider two different cases for emulation: a "main" ~~scheme~~ case which includes just the ACC, MBS, and MOS modes, and a "gCCN" (giant CCN) scheme which adds in ~~the~~ dust and sea salt modes. ~~All the~~ We treat these two cases separately because of the non-linear influence of gCCN on activation dynamics and cloud microphysics, which critically depends on the ambient CCN burden (Feingold et al., 1999).

For emulation, all the aerosol size distribution parameters are transformed using a logarithm, since they can take on values that span several orders of magnitude. ~~Additionally, we consider the hygroscopicity of the mixed sulfate-organic carbon mode, as well as the updraft speed and ambient temperature and pressure in our input parameter space.~~

~~For each of these parameters we construct uniform size distributions , which are uniquely defined by a set of low and high bounds. These bounds are also noted in Table 2, along with the percentile of the data they correspond to from our sampling study of the parameter space for the aerosol parameters. For most of those parameters, the bounds cover upwards of 99% of the sampled parameter space. Notably, the lower cut-off boundaries for dust and sea salt number concentration occur at much higher percentiles; the number concentration of droplets nucleated in our calculations is relatively insensitive to changes in the coarse mode number concentration at very low values, though, so we opt to constrain the input parameter space to these modes to a more physically relevant range. The MOS hygroscopicity, temperature, pressure, and updraft velocity ranges cover all plausible values that could be used in an online activation calculation within MARC.~~

~~We~~ We then construct uniform distributions with the associated ranges of values for each transformed parameter (Table 1). Using these uniform distributions, we cast all of the input parameters as independent random variables with a uniform probability density ~~functions to emphasize that we care equally about computing activation with a parameter set drawn with any parameter values~~function covering the range of each corresponding distribution.

This methodology represents a compromise between using high-fidelity representation of the aerosol size distribution parameters for our emulation, and the desire to build an emulator that can later be used in a GCM. However, ~~in MARC, some combinations of parameters are extremely unlikely~~we note that the distributions of aerosol parameters simulated by MARC are neither normal nor independent from one another. For instance, ~~sea salt has sources far removed spatially from the sources of black carbon; ergo, it is uncommon to see a high number concentration for sea salt as well as the mixed sulfate-black carbon mode. The~~ over remote maritime regions, total aerosol number concentration tends to be small but dominated by

sea salt and small sulfate particles. In contrast, continental regions with anthropogenic emissions may feature much higher burdens of carbonaceous aerosol. Using both numerically-generated orthogonal polynomials and statistical transformations, both of these complications can be handled directly (Isukapalli, 1999; Feinberg and Langtangen, 2015), but not without a trade-off~~here potentially lies in emulator performance, because the PCM will attempt to train the emulatorto perform well for input parameters that we've assigned equal likelihood to, but may actually be far less likely to occur. A major benefit from this trade-off is simplicity in matriculating the emulator for use in a GCM. Using multiple probability density functions for different input variables, while offering a tuning knob to increase the accuracy of the emulators, would require a larger set of orthogonal polynomial bases than just the Legendre polynomials used for the uniform distributions here.~~. First, regions of the multi-dimensional input parameter space with low but non-zero probability of occurrence are unlikely to be sampled when building the emulator. For a sufficiently linear response function, this may not be an issue. More importantly, it becomes difficult to serialize the resulting chaos expansion in a form that can be re-produced for use later. This requires storing both the weights (coefficients) of the numerically-generated orthogonal polynomials from the chaos expansion and some representation of how to re-construct the transformed joint probability distribution formed from the input parameter probability distributions. Employing uniform probability distributions for each input parameter and assuming independence solves both of these problems, since canonical orthogonal polynomials with well-known techniques to efficiently generate them can be used, and few additional, costly transformations of the parameter samples are necessary to run the emulator. We study the impact of this choice by evaluating samples of input parameter sets drawn from their true joint probability distribution (as simulated by MARC) in Section 3.

These parameters are used to drive parcel model simulations where we record ~~the logarithm of $S_{\max}$~~ $\log_{10} S_{\max}$ as the response variable. This value can then be used to diagnose the number concentration of droplets nucleated by assuming that any particles which experience their Köhler theory-predicted critical supersaturation activate. We note that although this does not resolve the issue of kinetic limitations on droplet growth and its potential to cause an under-prediction in droplet number (Nenes et al., 2001), unlike existing activation schemes, our emulator accounts for the feedback of these effects on $S_{\max}$, so one avenue of its impact is lessened.

~~Furthermore, emulators predicting $S_{\max}$ were much more accurate at reproducing parcel model behavior than those which directly predicted estimates of N_{act} accounting for kinetic limitations on growth.~~

The ~~end result of constructing the emulators is a function which maps~~ emulators constructed through this process are functions which map $\log_{10}(S_{\max})$ to a set of values from our input parameter space,

$$\begin{aligned}\log_{10}(S_{\max}) = f(&\log_{10} N_{\text{ACC}}, \log_{10} N_{\text{MOS}}, \log_{10} N_{\text{MBS}},\\ &\log_{10} \mu_{\text{ACC}}, \log_{10} \mu_{\text{MOS}}, \log_{10} \mu_{\text{MBS}}, \kappa_{\text{MOS}}, \log_{10} V, P, T[, m\\ &\log_{10} N_{\text{DST01}}, \log_{10} N_{\text{DST02}}, \log_{10} N_{\text{SSLT01}}])\end{aligned} \tag{3}$$

From a prediction of the $S_{\max}$ achieved in an ascending parcel with the conditions passed to the emulator, we can then diagnose aerosol activation by re-writing the lognormal size distribution for each mode as a function of critical supersaturation (Ghan et al., 2011) to yield an expression

$$N_{\text{act}} = \sum_{i=1}^{n} \frac{N_{t,i}}{2} \left(1 - \text{erf}\left[2\ln\left(\frac{S_{m,i}}{S_{\max}}\right) / (3\sqrt{2}\ln\sigma_{g,i})\right]\right) \tag{4}$$

where $S_{m,i}$ is the critical supersaturation for a particle of radius $\mu_{g,i}$ from mode i.

3 Evaluation of Emulators

We evaluate our emulators by applying them to both a synthetic sample of ~~potential~~ input parameters as well as real samples ~~taken~~ drawn from a MARC simulation. In all of our comparisons, we study third and fourth order chaos expansions both excluding ("main") and including ("gCCN") the coarse dust and sea salt modes.

As a reference, we compute activation statistics for each sample ~~from several different sources. First, we run the detailed parcel which the emulator aims to simulate. Second, as a further benchmark and comparison, we run~~ using both a detailed parcel model and two widely-used activation ~~parameterizations from the literature~~schemes. The first ~~scheme~~parameterization, by Abdul-Razzak and Ghan (2000) (ARG), uses a pseudo-analytical solution to an integro-differential equation derived from the original adiabatic parcel model system~~. However, one part of the pseudo-analytical calculation involves a fit to parcel model calculations. The secondparameterization~~; the second, by Morales Betancourt and Nenes (2014b) (MBN), applies an iterative scheme to partition the aerosol population into two subsets, and uses different limits on the underlying analytical formulas to derive a maximum supersaturation. Because it requires a sequence of iterations to run, the MBN scheme is more computationally expensive than the ARG scheme, but has the potential to include more detailed links between particle composition and condensation (Kumar et al., 2009) or entrainment into the parcel (Barahona and Nenes, 2007). ~~Like the ARG scheme, though, one limiting case in the MBN scheme relies on a~~ Both the ARG and MBN schemes rely on some parameters fit to parcel model simulations ~~. In both cases, those simulations involved models conceptually similar~~ conceptually similar (but different in implementation) to the one emulated here.

3.1 Input Parameter Space Sampling

Using the parameter space defined in Table 2, ~~$n = 10000$~~ $n = 10{,}000$ sample parameter sets were drawn using maximin Latin Hypercube Sampling (LHS). This randomized sampling method helps to ensure that the full aerosol and meteorology parameter space is studied while assessing its performance.

Figure 4 compares the performance of each emulator and the two reference activation scheme against parcel model simulations using all of the LHS samples for the "main" aerosol parameter sets. In the simulations, higher updraft speeds ~~(shaded)~~ are nearly always associated with a much higher supersaturation maximum. For the emulators, accuracy tends to increase on average going from the 3rd order (Fig. 4-a) to the 4th order (Fig. 4-b) scheme, although there is ~~slightly~~ higher variance in the

relative error compared to the parcel model at higher updraft speeds. With respect to the driving updraft speed, though, there isn't a consistent mode of bias~~--~~on average, the relative error is very low. The same does not hold true for the two reference schemes. The ARG scheme (Fig. 4-c) tends to ~~predict both too-high and too-low~~ mis-predict supersaturation maxima at higher updraft speeds but is relatively well-calibrated at lower updraft speeds, yielding a lower supersaturation maximum. On the other hand, the MBN scheme (Fig. 4-d) is ~~generally~~ more accurate and better-calibrated than either of the emulators or the ARG scheme, especially at higher updraft speeds~~--~~, but tends to spuriously over-estimate $S_{\max}$ for weak updraft speeds.

Figure 5 ~~takes the results depicted in Fig. 4 one step further by diagnosing droplet number concentrations nucleated from each~~ extends this evaluated to diagnosed CDNC (N_{act}) nucleated for each predicted $S_{\max}$. For all the schemes, there can be substantial differences between the parcel model and each parameterization. This is particularly the case in regimes which ~~give rise to fewer overall droplet number concentrations~~produce smaller total CDNC, either due to a lower driving updraft velocity, or a lower total aerosol number available to activate. ~~Surprisingly, the~~ The MBN scheme tends to consistently ~~activate~~ nucleate a higher number of droplets~~--~~, such as those where the total aerosol concentration is below $10\,\mathrm{cm}^{-3}$. ~~The ARG scheme~~ Although it does not have as consistent of a bias, ~~but~~ the ARG scheme can both egregiously over-predict and under-predict ~~droplet number~~CDNC, with these biases exaggerated at lower updraft speeds. By comparison, the emulators show much less overall bias. The mean error for the emulators follows that of $S_{\max}$ and is small, but there is variance which tends to impart a small low or high bias on its estimates.

Both of these sets of plots are repeated in Figs. 6 and 7, but for the "gCCN" experiment. Qualitatively, the results for all parameterizations are very similar, with the same overall biases - especially for the ARG and MBN parameterizations. The emulators tend not to perform as well overall in the "gCCN" cases, although they are still the most highly-calibrated scheme and do not have the velocity-regime errors that the MBN scheme has. In both the "main" and "gCCN" parameter sets, the MBN scheme tends to more regularly predict too many cloud droplets, save for polluted regimes giving rise to $100\,\mathrm{cm}^{-3}$ droplets where that bias reverses and the scheme has a tendency to under-predict droplet number. Neither the emulators nor the ARG show this same tendency in bias.

These differences in bias are most likely related to the choice of parcel model used in testing and building the ARG and MBN schemes; because each scheme relies on some empirical tuning to parcel model calculations, details in the implementation of each parcel model which influence its sensitivity should show up ensemble evaluations of each activation scheme. The "gCCN" case is more taxing to simulate with parcel models using a Lagrangian description of the particle size distribution, because condensational growth is computed for each particle bin simultaneously. The stiffness ratio in this case will be extremely large, as the liquid water uptake by small particles in the main aerosol modes ~~will grow much more slowly~~ is much slower than those in the giant CCN modes. Although modern ODE solvers can automatically handle these scenarios, the subjective choice of which particular solver and how to discretize the giant CCN population (how many bins per mode) could ~~greatly~~ influence the sensitivity of $S_{\max}$ to changes in the model inputs and account for the differences observed here.

To better summarize the results in Figs. 4 to 7, summary statistics on the error of each scheme versus their corresponding parcel model calculations are shown in Table 3. In both sampling cases, all of the parameterizations show a strong linear

correlation (r^2) between their predictions and the result of the parcel model. The emulators (PCM Order p) predict $S_{\max}$ with lower overall absolute and relative error, but with a much higher variance (not shown here). However, that lower error does not always translate into the emulators being the most accurate absolute predictors of N_{act}. For the "gCCN" parameters, the ARG scheme predicts N_{act} with a lower average mean relative error. In both parameter sets, the MBN scheme is the least accurate compared to the parcel model used in these sampling calculations.

3.2 MARC Aerosol Sampling

Although the sampling in the previous section fully exhausts the input parameter space over which aerosol activation may need to be assessed, it undoubtedly samples from aerosol and meteorological conditions which may not be likely to occur in the real world. To better understand the performance and potential bias of the emulators developed here and the existing activation schemes, then, we also studied a sample of ~~$n = 10000$~~ $n = 10{,}000$ aerosol and meteorology parameter sets drawn directly from ~~a MARC simulation .~~ the MARC simulation previously used to study the distributions of simulated aerosol parameters, in contrast with the previous LHS sample. Error statistics from this sample, since they use model-produced parameter sets, are more representative of the real-world performance of the emulators and physically-based activation schemes. All of the schemes were evaluated again using these parameter sets and the same detailed parcel model. This includes the "main" and "gCCN" emulators, which allows us to identify the importance of including the dust and sea salt modes as predictors in the chaos expansions. The parameters in these sets occasionally include values outside the ranges defined in Table 2 and studied in the previous section. These cases are more frequently associated with very low total aerosol number concentration, especially over the ocean where anthropogenic aerosols are limited and natural aerosols ~~—~~ which have a lower overall number burden ~~—~~ dominate. Because the distributions of the parameters of aerosol samples from oceanic and continental grid cells differ in this fundamental way, we break down the following analysis to reflect those differences. As in the previous sampling experiment, summary statistics on the performance of each emulator, alongside the ARG and MBN schemes, are detailed in Table 4.

Qualitatively, all of the activation schemes perform similarly when evaluated against the MARC parameters as compared to the more generic sampling in the previous section. Figure 8 summarizes distributions of relative error in N_{act} over land and ocean for each scheme. Neither the ARG nor the MBN scheme show much difference in error for the two regimes, although on average, the MBN tends to under-predict N_{act}. This under-prediction usually occurs in regimes with higher updraft speeds and thus higher overall droplet number concentrations. In conditions with weaker updraft speeds, the MBN scheme instead tends to slightly over-predict N_{act}. The ARG scheme is ~~particularly~~ well-calibrated in both regimes.

The emulators derived here do not fare as well as the physically-based parameterizations when using the MARC samples. Both 3rd order schemes tend to over-predict droplet number over oceans, and under-predict it over land, but with an extremely large variance extending to $\pm 100\%$. However, including the effects of giant CCN measurably improves the performance of the 3rd order emulators in oceanic regimes. Increasing the order of the emulator also has a significant impact on their accuracy; the 4th order scheme which neglects giant CCN ~~actually out-performs~~ produces smaller absolute error than the ARG and MBN ~~scheme~~ schemes on average, and shows little bias between land and ocean regimes, indicating good convergence with its parent parcel model. On the other hand, the gCCN scheme has not yet converged by including 4th order terms, even while its mean

error statistics improve. Particularly troublesome is a secondary mode of extreme ~~(over 100%)~~ under-prediction of droplet number of oceanic regimes, but this metric is deceptive. ~~Really, what is occurring is that for~~ For very low total aerosol number concentrations~~,~~ with particle number in the single-digits per cubic centimeter~~,~~ the 4th order "gCCN" scheme tends to predict half as many droplets as parcel model calculations indicate should form. This typically occurs when one or more of the input size distribution parameters (in particular, the number concentration) for the natural aerosol ~~dips~~ falls below the minimum threshold where the emulator was trained. When the emulators encounter inputs greater (lower) than these thresholds, they hold them to the maximum (minimum) value in its training range. This follows the assumption that the bounds for each parameter cover the entire range over which activation is sensitive to changes in that input. ~~Put another way~~ As a result, activation should be relatively insensitive to changes near the maximum or minimum values in the range for each parameter. With respect to number concentration, this must be the case; populations with fewer than 10^{-3} particles cm^{-3} offer very little surface area for condensation and water vapor sink, and simply cannot exert a strong influence over the developing supersaturation in the parcel. That the 4th order "gCCN" emulator produces too high of sensitivity in this regime suggests that statistical over-fitting is occurring near the extremes of the input parameter space.

To contextualize these differences in N_{act} bias over different geographical regimes, Fig. 9 re-maps the testing samples back to the original MARC grid. Here, the difference in regional biases becomes much clearer. Virtually everywhere, the MBN scheme is biased a little low, but there is no systematic difference in this bias between land or ocean, or by geographical areas. The ARG scheme and the 4th order "main" scheme show a different pattern; the ocean-land contrast in bias is clearly visible in the northern hemisphere. Furthermore, the bias is typically positive over maritime regions, but negative over regions with anthropogenic aerosol influence. In particular, these regions include Europe and southeastern Asia - where aerosol distributions are dominated by anthropogenic sulfate and black carbon - and over north central Africa - where the aerosol is a mixture of both dust and organic carbon emissions from biomass burning. In the zonal average, the main_4 scheme is virtually identical to the ARG scheme. However, both cases as well as with MBN, there are larger biases over the southern parts of the oceans, where the aerosol is predominantly comprised of sea salt and smaller sulfate particles produced indirectly through the emission of DMS.

Figure 9 also illustrates the poor performance of the gCCN_4 scheme, which under-predicts N_{act} nearly everywhere, but especially so in the southern portions of the ocean basins. The consistent under-prediction in this region explains the bimodal distribution over the ocean hinted at in Fig. 8. The gCCN_4 scheme does not perform too dissimilarly than the other schemes over regions with anthropogenic pollution or with mostly dust aerosol.

3.3 Implementation in MARC and Computational Expense

The ARG scheme is the original activation parameterization used within CAM5.3 to assess cloud droplet nucleation. We implemented the MBN scheme as an alternative in MARC, as well as an interface for chaos expansion-based schemes. To use the emulators derived in this work, one must provide a NetCDF file which contains at least three pieces of information:

- an m-length vector of coefficients corresponding to each of the m terms in the expansion

- a 2×p-shape matrix which defines the lower and upper bounds for each of the input parameters
- a $m \times p$ matrix of integers correspond to the p variable expansion orders for each of the m terms in the expansion

MARC caches these vectors and matrices in memory at start-up, just as it caches several time-invariant terms used in both the ARG and the MBN schemes for each of the CCN-providing aerosol modes.

To estimate the impact of each scheme on MARC's performance, we performed a set of three-month simulations initialized with fully spun-up aerosol and meteorology fields from a previous experiment. The simulations were conducted using 480 MPI tasks with two threads allocated to each task. Using the default configuration of MARC with the ARG scheme, the atmosphere component of the model averaged 6.1 s per model day. The MBN scheme averaged 7% longer per model day, while the emulators tended to be comparable to the ARG scheme. Per model day, both the "main" schemes were comparable to within 0.4% of the ARG scheme's performance, with the higher-order scheme costing an additional 0.16%. Similarly, the "gCCN" schemes also compared similarly with the ARG scheme; the 3rd-order scheme 0.15% faster than the ARG scheme, but the 4th-order scheme was 3% slower.

Adding additional parameters to the chaos expansion underpinning the emulators would continue to add overhead to each evaluation by increasing the number of terms in the expansion. However, a larger penalty is incurred by increasing the expansion order for a given set of parameters, because this produces a much larger increase in the number of terms added to the expansion than adding a single parameter for the same order expansion. An assessment of the offline implementations of each scheme used in the analysis in the previous section yielded similar results.

4 Discussion and Conclusions

In this work, we ~~extended the meta-modeling~~ extend the metamodeling technique of Rothenberg and Wang (2016) in order to ~~apply it to assess aerosol~~ assess activation of a complex, multi-modal aerosol mixture simulated by a modern aerosol-climate model. Simultaneously, we characterize the performance of both our new emulators for aerosol activation and two widely-used schemes from the literature, focusing on that same high-dimensional, complex aerosol parameter space. To identify the most important factors impacting activation in that complex parameter space, we apply a physically-based approach to assess the sensitivity of activation statistics to the composition of the aerosol size distribution. Finally, we explore contrasts between aerosol and meteorology regimes over land and ocean, noting the potential for different biases in assessed cloud droplet number depending on the choice of activation scheme used in a particular global modeling application.

In ensembles of iterative calculations using a large sample of aerosol size distributions from a coupled aerosol-climate model, we note that typically, a single mode tends to dominate activation or otherwise strongly predict the total number of droplets nucleated. This approach to understanding the sensitivities of activation dynamics on the underlying aerosol population is distinct from previously-published approaches in the literature. For instance, Karydis et al. (2012) and Morales Betancourt and Nenes (2014a) apply an adjoint approach to derive the sensitivity of aerosol activation to perturbations in input parameters supplied to activation schemes. Detailed calculations using this approach yield a map of local sensitivities or gradients in the

relationship between, for example, N_{act} and one input parameter while holding all others constant, and are thus difficult to interpret. The iterative calculations performed here aim instead to address the global sensitivity of activation to configurations of an aerosol population.

~~It is somewhat surprising that~~ In terms of predicting CDNC, the accumulation mode sulfate (ACC) ~~successfully serves as such a strong~~ alone serves as a good proxy for the activity of a full aerosol population ~~, even~~ in many cases, including in the presence of giant CCN and a wide swath myriad updraft regimes. However, it is known that giant CCN exert a larger influence on precipitation formation in cleaner regimes (Feingold et al., 1999; Yin et al., 2000), and thus where ACC is abundant (especially over continents) the impacts of giant CCN on N_{act} can be muted. This result is ~~likely~~ also model-dependent in some sense; the ACC mode in MARC is not only ubiquitous, but may ~~be~~ inadvertently (and subjectively) ~~in~~ take a range of mean particle sizes for which aerosol activation is especially sensitive. At the same time, the coarse dust and sea salt modes in MARC, on average, hold too small a number concentration to dramatically impact activation calculations save for remote maritime regions far removed from anthropogenic sources. However, the presence of sea salt as one of the modes most frequently ranked in the top three influencers of activation ~~points to~~ agrees with previous results which indicate the presence of giant CCN can influence activation dynamics (e.g. Barahona et al., 2010).

The fact that a single mode can place such a strong constraint on aerosol activation is useful for attempts seeking to extend look-up table methods for building parameterizations. If two modes—an accumulation-size and a coarse-size—accurately predict aerosol activation, then one can constrain the look-up table to just a few key aerosol size distribution parameters. The inclusion of variable aerosol composition would still likely make employing a look-up table in a global model unwieldy, though, necessitating more sophisticated approaches ~~. The emulation technique applied hereis one such approach to tackling this problem which appears to work very well~~such as the metamodeling technique adopted here.

When sampling against the full training parameter space~~employed here~~, our emulators perform capably. Neglecting the influence of the giant CCN modes, the ~~emulators built average a~~ mean relative error ~~of~~ in predicting $\log_{10} S_{max}$ for the emulators is less than 1% ~~in predicting $\log_{10} S_{max}$~~, which translates to ~~an mean relative error~~ mean relative errors for $N_{act}$of 9.2% and 8.9%~~in predicting N_{act}~~. Including the giant CCN mode appears, at first, to dramatically increase the performance of the emulator, bringing those same metrics down to 0.3% and 6.9% for the 4th-order scheme. Relative to the ARG and MBN schemes, the emulators are much more accurate on average when compared to our reference parcel model. ~~However, we note that both the ARG and MBN schemes contain components which themselves are tuned to parcel models employed by their developers. Thus, we should not expect those schemes to perfectly match the parcel model results calculated here.~~ Instead, we emphasize that the comparison of our emulators with the ARG and MBN scheme is motivated as part of a broader attempt to understand how the fundamental activation process ~~initiates a chain of physics which ultimately lead to the aerosol indirect effect on climate.~~dictates the simulated relationship between aerosol burden and CDNC in a global climate model. This relationship is critical for understanding uncertainty in the indirect effect produced by any given model, since the simulated background CDNC strongly correlates with its strength (Hoose et al., 2009).

Assessing the relative performance of activation schemes which, for all intents and purposes, perform extremely well at reproducing their own reference parcel models, is a critical step in establishing the parametric uncertainty in translating aerosol to droplet numbers and which underlies uncertainty in global model estimates of the indirect effect.

For this reason, we supplemented the evaluation of our emulators by using a second set of input parameter samples drawn from aerosol fields simulated by an aerosol-climate model. In contrast with previous studies, we use instantaneous fields in lieu of monthly or annual averages for our samples. Activation is inherently a fast process; because the microphysics schemes in aerosol-cloud models directly account for a tendency of new droplets formed via nucleation, the activation parameterization in any model will be called every time-step and ~~for~~ in every grid-cell where clouds are occurring. Assessing activation schemes using temporally-averaged aerosol fields risks missing some combinations of input parameters and limiting the range of values for which the scheme will need to accurately perform.

Most of the emulators and schemes tested here perform ~~somewhat differently over land and ocean~~differently in oceanic and continental regimes, owing to the ~~presence (or lack thereof)~~ relative abundance of natural and anthropogenic aerosols in ~~these different regimes. Unfortunately, when~~ each. When focusing on the narrower range of aerosol parameters present in MARC (in comparison with the larger parameter space on which the emulators were trained), the emulators which explicitly account for giant CCN perform poorly, especially ~~over ocean~~ in maritime regimes dominated by sea salt. However, their counterpart performs nearly identical to the ARG scheme, showing a slight over-prediction of N_{act} in maritime regimes and a slight under-prediction over continents. In the global average, the emulator agrees better with the detailed parcel model than the ARG scheme. By comparison, the MBN scheme, while prone to under-predicting N_{act} in both regimes in these calculations, shows far less variance in its mis-prediction. This would suggest the MBN scheme actually performs extremely well~~--~~it is simply calibrated against a different baseline~~(in this case, a different parcel model).~~. Both the ARG and MBN schemes were developed using parcel models conceptually-similar to the one employed here, but which differ in the details of their implementation. Furthermore, both schemes use some parameters computed from empirical fits to their associated parcel models. As a result, we do not expect perfect agreement between all the schemes evaluated her, and instead note the importance of the relative differences between the CDNC simulated for each one. In particular, the MBN scheme does not show a large difference in relative error versus our parcel model between ocean and land regions, suggesting it is appropriately sensitive to a large range of different aerosol populations.

The results presented here have important implications for global modeling studies seeking to quantify ~~uncertain~~ uncertainty in the aerosol indirect effect on climate. While different activation schemes generally perform equally well when faced with idealized sets of input parameters (Ghan et al., 2011), their application in coupled aerosol-climate models may not be straightforward. Relative to parcel model calculations, activation schemes can likely show biases in predicting cloud droplet number in different regions of the world owing to spatial heterogeneity in the underlying aerosol and meteorology parameter distributions. This, in turn, ~~will~~ could lead to biases in cloud radiative forcing and diagnosis of the indirect effect.

~~Some literature has already implicated the role of activation schemes in divergent model estimates of the indirect effect.~~ For instance, Ghan et al. (2011) performed a pair of GCM experiments using two different schemes and ~~noted that between their simulations there is~~ observed a 10% difference in the global average ~~droplet number concentration, which produces~~ CDNC,

which produced a $0.2\,\mathrm{W\,m^{-2}}$ difference in the indirect effect. ~~Using a sequence of increasingly-complex activation schemes, Gantt et al. (2014) performed similar simulations with just a present-day emissions scenario, showing~~ Gantt et al. (2014) similarly showed large regional differences in ~~average cloud droplet number concentration and, as a result, up to a difference of~~ CDNC when using a different set of activation schemes, leading to a spread $0.9\,\mathrm{W\,m^{-2}}$ in global average shortwave cloud forcing. ~~This perturbation in forcing naturally follows from results such as those highlighted in this work; changes in the base cloud droplet number concentration simulated in an aerosol-climate model have important consequences for the chain of cloud microphysical processes which ultimately give rise to the indirect effect . Those biases~~ These impacts on CDNC and indirect effect resulting from using different activation schemes will necessarily be model-dependent, since the formulation of the basic activation diagnostic in each model is intertwined with regional and global variability in their simulated aerosol size distributions.

Future work should seek to systematically assess the differences in cloud microphysical processes and aerosol-cloud interactions arising from choice of activation schemes in aerosol-climate models. As this work illustrates, employing emulators of detailed parcel model calculations ~~including various~~ which include complex chemical and physical effects on ~~the activation process~~ activation will aid with this task, ~~providing a way to quickly account for myriad facts which may be difficult or impossible to include in existing activation schemes or frameworks~~since additional effects (changes in droplet surface tension due to organic surfactants (Abdul-Razzak and Ghan, 2004)) can more easily be incorporated into parameterizations built using this method. However, this work must proceed in tandem with efforts to place strong constraints on the climatology and variability of cloud droplet number concentration across regions and meteorological regimes. The synthesis of these two lines of work may provide the necessary constraints to diagnose systematic biases in the representation of fundamental aerosol-cloud interactions in global aerosol-climate models and thus reconcile the disagreement between model- and satellite-derived estimates of the indirect effect.

Appendix A: Code and Data Availability

A git repository archiving the scripts used to generate the chaos expansions can be found at https://github.mit.edu/darothen/marc_pcm_activation. For the convenience of the reader, an up-to-date commit (c71f8ca9bd4) has been included in the Supplementary Materials. Dependencies of these scripts are recorded in the README file therein. The sampling datasets generated for analysis in this work are archived with DOI 10.5281/zenodo.60937. The source code and documentation for the pyrcel cloud parcel model are archived with DOI 10.5281/zenodo.46127, and can be accessed from http://github.com/darothen/pyrcel.

Acknowledgements. The work in this study was supported by the National Science Foundation Graduate Research Fellowship Program under both NSF Grant 1122374 and NSF Grant AGS-1339264; the National Research Foundation of Singapore through the Singapore–MIT Alliance for Research and Technology and the interdisciplinary research group of the Center for Environmental Sensing and Modeling; and the U.S. Department of Energy, Office of Science (DE-FG02-94ER61937). We thank Steve Ghan (PNNL) and Athanasios Nenes (Georgia Tech) for reference implementations of their activation parameterizations. We would also like to thank ~~Topical Editor Graham Mann~~ Graham Mann and three anonymous reviews for comments that helped improve this manuscript.

References

Abdul-Razzak, H.: A parameterization of aerosol activation 3. Sectional representation, Journal of Geophysical Research, 107, 4026, doi:10.1029/2001JD000483, http://www.agu.org/pubs/crossref/2002/2001JD000483.shtmlhttp://doi.wiley.com/10.1029/2001JD000483, 2002.

Abdul-Razzak, H. and Ghan, S. J.: A parameterization of aerosol activation 2. Multiple aerosol types, Journal of Geophysical Research, 105, 6837, doi:10.1029/1999JD901161, http://www.agu.org/pubs/crossref/2000/1999JD901161.shtmlhttp://dx.doi.org/10.1029/1999jd901161, 2000.

Abdul-Razzak, H. and Ghan, S. J.: Parameterization of the influence of organic surfactants on aerosol activation, Journal of Geophysical Research: Atmospheres, 109, n/a–n/a, doi:10.1029/2003JD004043, http://doi.wiley.com/10.1029/2003JD004043, 2004.

Abdul-Razzak, H., Ghan, S. J., Rivera-Carpio, C., Razzak, H. A., and Carpio, C. R.: A parameterization of aerosol activation: 1. Single aerosol type, Journal of Geophysical Research, 103, 6123, doi:10.1029/97JD03735, http://www.agu.org/pubs/crossref/1998/97JD03735.shtmlhttp://doi.wiley.com/10.1029/97JD03735, 1998.

Adams, B. M., Ebeida, M. S., Eldred, M. S., Jakeman, J. D., Swiler, L. P., Stephens, J. A., Vigil, D. M., Wildey, T. M., Bohnhoff, W. J., Dalbey, K. R., Eddy, J. P., Hu, K. T., Bauman, L. E., and Hough, P. D.: DAKOTA, A Multilevel Parallel Object-Oriented Framework for Design Optimization, Parameter Estimation, Uncertainty Quantification, and Sensitivity Analysis: Version 6.0 User's Manual, Tech. rep., Sandia National Laboratories, Albuquerque, New Mexico, 2014.

Albani, S., Mahowald, N. M., Perry, A. T., Scanza, R. A., Zender, C. S., Heavens, N. G., Maggi, V., Kok, J. F., and Otto-Bliesner, B. L.: Improved dust representation in the Community Atmosphere Model, Journal of Advances in Modeling Earth Systems, pp. n/a–n/a, doi:10.1002/2013MS000279, http://doi.wiley.com/10.1002/2013MS000279, 2014.

Barahona, D. and Nenes, A.: Parameterization of cloud droplet formation in large-scale models: Including effects of entrainment, Journal of Geophysical Research, 112, D16 206, doi:10.1029/2007JD008473, http://doi.wiley.com/10.1029/2007JD008473, 2007.

Barahona, D., West, R. E. L., Stier, P., Romakkaniemi, S., Kokkola, H., and Nenes, A.: Comprehensively accounting for the effect of giant CCN in cloud activation parameterizations, Atmospheric Chemistry and Physics, 10, 2467–2473, doi:10.5194/acp-10-2467-2010, http://www.atmos-chem-phys.net/10/2467/2010/, 2010.

Boucher, O. and Lohmann, U.: The Sulfate-Ccn-Cloud Albedo Effect - a Sensitivity Study With 2 General-Circulation Models, doi:10.1034/j.1600-0889.47.issue3.1.x, 1995.

Boucher, O., Randall, D., Artaxo, P., Bretherton, C. S., Feingold, G., Forster, P., Kerminen, V.-M., Kondo, Y., Liao, H., Lohmann, U., Rasch, P., Satheesh, S. K., Sherwood, S., Stevens, B., and Zhang, X. Y.: Clouds and Aerosols, in: Climate Change 2013: The Physical Science Basis. Contribution of Working Group I to the Fifth Assessment Report of the Intergovernmental Panel on Climate Change, edited by Stocker, T. F., Qin, D., Plattner, G.-K., Tignor, M., Allen, S. K., Boschung, J., Nauels, A., Xia, Y., Bex, V., and Midgley, P. M., chap. 7, pp. 571–657, Cambridge University Press, Cambridge, United Kingdom, and New York, NY, USA, 2013.

Carslaw, K. S., Lee, L. a., Reddington, C. L., Pringle, K. J., Rap, a., Forster, P. M., Mann, G. W., Spracklen, D. V., Woodhouse, M. T., Regayre, L. a., and Pierce, J. R.: Large contribution of natural aerosols to uncertainty in indirect forcing., Nature, 503, 67–71, doi:10.1038/nature12674, http://www.ncbi.nlm.nih.gov/pubmed/24201280, 2013.

Cohard, J.-M. and Pinty, J.-P.: A comprehensive two-moment warm microphysical bulk scheme. I: Description and tests, Quart. J. Roy. Meteor. Soc., 126, 1815–1842, doi:10.1002/qj.49712656613, http://doi.wiley.com/10.1002/qj.49712656614, 2000.

Cohard, J.-M., Pinty, J.-P., and Bedos, C.: Extending Twomey's Analytical Estimate of Nucleated Cloud Droplet Concentrations from CCN Spectra, Journal of the Atmospheric Sciences, 55, 3348–3357, doi:10.1175/1520-0469(1998)055<3348:ETSAEO>2.0.CO;2, 1998.

Ervens, B., Feingold, G., and Kreidenweis, S. M.: Influence of water-soluble organic carbon on cloud drop number concentration, Journal of Geophysical Research D: Atmospheres, 110, 1–14, doi:10.1029/2004JD005634, 2005.

Feinberg, J. and Langtangen, H. P.: Chaospy: An open source tool for designing methods of uncertainty quantification, Journal of Computational Science, 11, 46–57, doi:10.1016/j.jocs.2015.08.008, http://linkinghub.elsevier.com/retrieve/pii/S1877750315300119, 2015.

Feingold, G. and Heymsfield, A. J.: Parameterizations of Condensational Growth of Droplets for Use in General Circulation Models, Journal of the Atmospheric Sciences, 49, 2325–2342, http://journals.ametsoc.org/doi/abs/10.1175/1520-0469(1992)049{%}3C2325:POCGOD{%}3E2.0.CO;2, 1992.

Feingold, G., Cotton, W. R., Kreidenweis, S. M., and Davis, J. T.: The Impact of Giant Cloud Condensation Nuclei on Drizzle Formation in Stratocumulus: Implications for Cloud Radiative Properties, Journal of the Atmospheric Sciences, 56, 4100–4117, doi:10.1175/1520-0469(1999)056<4100:TIOGCC>2.0.CO;2, http://journals.ametsoc.org/doi/abs/10.1175/1520-0469{%}281999{%}29056{%}3C4100{%}3ATIOGCC{%}3E2.0.CO{%}3B2, 1999.

Feingold, G., Remer, L., Ramaprasad, J., and Kaufman, Y. J.: Analysis of smoke impact on clouds in Brazilian biomass burning regions: An extension of Twomey's approach, Journal of Geophysical Research, 106, 22 907, doi:10.1029/2001JD000732, http://doi.wiley.com/10.1029/2001JD000732, 2001.

Fountoukis, C. and Nenes, A.: Continued development of a cloud droplet formation parameterization for global climate models, Journal of Geophysical Research, 110, D11 212, doi:10.1029/2004JD005591, http://www.agu.org/pubs/crossref/2005/2004JD005591.shtml, 2005.

Fountoukis, C., Nenes, A., Meskhidze, N., Bahreini, R., Conant, W. C., Jonsson, H., Murphy, S., Sorooshian, A., Varutbangkul, V., Brechtel, F., Flagan, R. C., and Seinfeld, J. H.: Aerosol–cloud drop concentration closure for clouds sampled during the International Consortium for Atmospheric Research on Transport and Transformation 2004 campaign, Journal of Geophysical Research, 112, D10S30, doi:10.1029/2006JD007272, http://doi.wiley.com/10.1029/2006JD007272, 2007.

Gantt, B., He, J., Zhang, X., Zhang, Y., and Nenes, A.: Incorporation of advanced aerosol activation treatments into CESM/CAM5: Model evaluation and impacts on aerosol indirect effects, Atmospheric Chemistry and Physics, 14, 7485–7497, doi:10.5194/acp-14-7485-2014, http://www.atmos-chem-phys.net/14/7485/2014/, 2014.

Ghan, S. J., Leung, L. R., Easter, R. C., and Abdul-Razzak, H.: Prediction of cloud droplet number in a general circulation model, Journal of Geophysical Research: Atmospheres, 102, 21 777–21 794, doi:10.1029/97JD01810, http://doi.wiley.com/10.1029/97JD01810, 1997.

Ghan, S. J., Abdul-Razzak, H., Nenes, A., Ming, Y., Liu, X., Ovchinnikov, M., Shipway, B., Meskhidze, N., Xu, J., and Shi, X.: Droplet nucleation: Physically-based parameterizations and comparative evaluation, Journal of Advances in Modeling Earth Systems, 3, M10 001, doi:10.1029/2011MS000074, http://dx.doi.org/10.1029/2011MS000074, 2011.

Ghan, S. J. S., Chung, C. C. C., and Penner, J. E. J.: A parameterization of cloud droplet nucleation part I: single aerosol type, Atmospheric Research, 30, 198–221, doi:10.1016/0169-8095(93)90024-I, http://www.sciencedirect.com/science/article/pii/016980959390024Ihttp://linkinghub.elsevier.com/retrieve/pii/016980959390024I, 1993.

Hoose, C., Kristjánsson, J. E., Iversen, T., Kirkevåg, a., Seland, Ø., and Gettelman, a.: Constraining cloud droplet number concentration in GCMs suppresses the aerosol indirect effect, Geophysical Research Letters, 36, L12 807, doi:10.1029/2009GL038568, http://doi.wiley.com/10.1029/2009GL038568, 2009.

Isukapalli, S. S.: Uncertainty analysis of transport-transformation models, Ph.D. thesis, Rutgers, The State University of New Jersey, 1999.

Jones, A., Roberts, D. L., Woodage, M. J., and Johnson, C. E.: Indirect sulphate aerosol forcing in a climate model with an interactive sulphur cycle, Journal of Geophysical Research: Atmospheres, 106, 20 293–20 310, doi:10.1029/2000JD000089, http://doi.wiley.com/10.1029/2000JD000089, 2001.

Karydis, V. A., Capps, S. L., Russell, A. G., and Nenes, A.: Adjoint sensitivity of global cloud droplet number to aerosol and dynamical parameters, Atmospheric Chemistry and Physics, 12, 9041–9055, doi:10.5194/acp-12-9041-2012, http://www.atmos-chem-phys.net/12/9041/2012/, 2012.

Khvorostyanov, V. I. and Curry, J. a.: Aerosol size spectra and CCN activity spectra: Reconciling the lognormal, algebraic, and power laws, Journal of Geophysical Research, 111, D12 202, doi:10.1029/2005JD006532, http://www.agu.org/pubs/crossref/2006/2005JD006532.shtml, 2006.

Kim, D., Wang, C., Ekman, A. M. L., Barth, M. C., and Rasch, P. J.: Distribution and direct radiative forcing of carbonaceous and sulfate aerosols in an interactive size-resolving aerosol–climate model, Journal of Geophysical Research, 113, D16 309, doi:10.1029/2007JD009756, http://www.agu.org/pubs/crossref/2008/2007JD009756.shtml, 2008.

Kim, D., Wang, C., Ekman, A. M. L., Barth, M. C., and Lee, D.-I.: The responses of cloudiness to the direct radiative effect of sulfate and carbonaceous aerosols, Journal of Geophysical Research: Atmospheres, pp. n/a–n/a, doi:10.1002/2013JD020529, http://doi.wiley.com/10.1002/2013JD020529, 2014.

Kumar, P., Sokolik, I. N., and Nenes, a.: Parameterization of cloud droplet formation for global and regional models: including adsorption activation from insoluble CCN, Atmospheric Chemistry and Physics, 9, 2517–2532, doi:10.5194/acp-9-2517-2009, http://www.atmos-chem-phys.net/9/2517/2009/, 2009.

Leaitch, W. R., Strapp, J. W., Isaac, G. A., and Hudson, J. G.: Cloud droplet nucleation and cloud scavenging of aerosol sulphate in polluted atmospheres, Tellus B, 38B, 328–344, doi:10.1111/j.1600-0889.1986.tb00258.x, http://www.tellusb.net/index.php/tellusb/article/view/15141, 1986.

Liu, X., Easter, R. C., Ghan, S. J., Zaveri, R., Rasch, P., Shi, X., Lamarque, J.-F., Gettelman, A., Morrison, H., Vitt, F., Conley, A., Park, S., Neale, R., Hannay, C., Ekman, a. M. L., Hess, P., Mahowald, N., Collins, W., Iacono, M. J., Bretherton, C. S., Flanner, M. G., and Mitchell, D.: Toward a minimal representation of aerosols in climate models: description and evaluation in the Community Atmosphere Model CAM5, Geoscientific Model Development, 5, 709–739, doi:10.5194/gmd-5-709-2012, http://www.geosci-model-dev.net/5/709/2012/, 2012.

Lohmann, U., Feichter, J., Chuang, C. C., and Penner, J. E.: Prediction of the number of cloud droplets in the ECHAM GCM, Journal of Geophysical Research, 104, 9169–9198, http://onlinelibrary.wiley.com/doi/10.1029/1999JD900046/full, 1999.

Mårtensson, E. M., Nilsson, E. D., de Leeuw, G., Cohen, L. H., and Hansson, H.-C.: Laboratory simulations and parameterization of the primary marine aerosol production, Journal of Geophysical Research: Atmospheres, 108, n/a–n/a, doi:10.1029/2002JD002263, http://doi.wiley.com/10.1029/2002JD002263, 2003.

Meskhidze, N.: Evaluation of a new cloud droplet activation parameterization with in situ data from CRYSTAL-FACE and CSTRIPE, Journal of Geophysical Research, 110, D16 202, doi:10.1029/2004JD005703, http://doi.wiley.com/10.1029/2004JD005703, 2005.

Ming, Y., Ramaswamy, V., Donner, L. J., and Phillips, V. T. J.: A New Parameterization of Cloud Droplet Activation Applicable to General Circulation Models, Journal of the Atmospheric Sciences, 63, 1348–1356, doi:10.1175/JAS3686.1, http://journals.ametsoc.org/doi/abs/10.1175/JAS3686.1, 2006.

Morales, R. and Nenes, a.: Characteristic updrafts for computing distribution-averaged cloud droplet number and stratocumulus cloud properties, Journal of Geophysical Research, 115, D18 220, doi:10.1029/2009JD013233, http://doi.wiley.com/10.1029/2009JD013233, 2010.

Morales, R., Nenes, A., Jonsson, H., Flagan, R. C., and Seinfeld, J. H.: Evaluation of an entraining droplet activation parameterization using in situ cloud data, Journal of Geophysical Research, 116, 1–9, doi:10.1029/2010JD015324, http://doi.wiley.com/10.1029/2010JD015324, 2011.

Morales Betancourt, R. and Nenes, A.: Understanding the contributions of aerosol properties and parameterization discrepancies to droplet number variability in a global climate model, Atmospheric Chemistry and Physics, 14, 4809–4826, doi:10.5194/acp-14-4809-2014, http://www.atmos-chem-phys.net/14/4809/2014/, 2014a.

Morales Betancourt, R. and Nenes, A.: Droplet activation parameterization: the population-splitting concept revisited, Geoscientific Model Development, 7, 2345–2357, doi:10.5194/gmd-7-2345-2014, http://www.geosci-model-dev.net/7/2345/2014/, 2014b.

Morrison, H., Gettelman, A., Morrison, H., and Ghan, S. J.: A New Two-Moment Bulk Stratiform Cloud Microphysics Scheme in the Community Atmosphere Model, Version 3 (CAM3). Part I: Description and Numerical Tests, Journal of Climate, 21, 3642–3659, doi:10.1175/2008JCLI2105.1, http://journals.ametsoc.org/doi/abs/10.1175/2008JCLI2116.1http://journals.ametsoc.org/doi/abs/10.1175/2008JCLI2105.1, 2008.

Neale, R. B., Gettelman, A., Park, S., Chen, C.-c., Lauritzen, P. H., Williamson, D. L., Conley, A. J., Kinnison, D., Marsh, D., Smith, A. K., Vitt, F., Garcia, R., Lamarque, J.-f., Mills, M., Tilmes, S., Morrison, H., Cameron-smith, P., Collins, W. D., Iacono, M. J., Easter, R. C., Liu, X., Ghan, S. J., Rasch, P. J., and Taylor, M. a.: Description of the NCAR Community Atmosphere Model (CAM 5.0). NCAR Technical Notes., Ncar/Tn-464+Str, p. 214, 2012.

Nenes, A. and Seinfeld, J. H.: Parameterization of cloud droplet formation in global climate models, Journal of Geophysical Research, 108, 4415, doi:10.1029/2002JD002911, http://www.agu.org/pubs/crossref/2003/2002JD002911.shtml, 2003.

Nenes, A., Ghan, S., Abdul-Razzak, H., Chuang, P. Y., and Seinfeld, J. H.: Kinetic limitations on cloud droplet formation and impact on cloud albedo, Tellus Series B-Chemical and Physical Meteorology, 53, 133–149, doi:10.1034/j.1600-0889.2001.d01-12.x, http://www.tellusb.net/index.php/tellusb/article/view/16569http://www.tellusb.net/index.php/tellusb/article/view/16569{%}5Cn{%}3CGotoISI{%}3E://WOS:000169810700003, 2001.

Park, S. and Bretherton, C. S.: The University of Washington shallow convection and moist turbulence schemes and their impact on climate simulations with the community atmosphere model, Journal of Climate, 22, 3449–3469, doi:10.1175/2008JCLI2557.1, 2009.

Partridge, D. G., Vrugt, J. a., Tunved, P., Ekman, a. M. L., Gorea, D., and Sorooshian, a.: Inverse modeling of cloud-aerosol interactions – Part 1: Detailed response surface analysis, Atmospheric Chemistry and Physics, 11, 7269–7287, doi:10.5194/acp-11-7269-2011, http://www.atmos-chem-phys.net/11/7269/2011/, 2011.

Petters, M. D. and Kreidenweis, S. M.: A single parameter representation of hygroscopic growth and cloud condensation nucleus activity, Atmospheric Chemistry and Physics, 7, 1961–1971, doi:10.5194/acp-7-1961-2007, http://www.atmos-chem-phys.net/7/1961/2007/http://www.atmos-chem-phys.net/13/1081/2013/acp-13-1081-2013.htmlhttp://www.atmos-chem-phys.net/13/1081/2013/, 2007.

Rothenberg, D. and Wang, C.: Metamodeling of Droplet Activation for Global Climate Models, Journal of the Atmospheric Sciences, 73, 1255–1272, doi:10.1175/JAS-D-15-0223.1, http://journals.ametsoc.org/doi/abs/10.1175/JAS-D-15-0223.1http://journals.ametsoc.org/doi/10.1175/JAS-D-15-0223.1, 2016.

Saleeby, S. M. and Cotton, W. R.: A Large-Droplet Mode and Prognostic Number Concentration of Cloud Droplets in the Colorado State University Regional Atmospheric Modeling System (RAMS). Part I: Module Descriptions and Supercell Test Simulations, Journal of Applied Meteorology, 43, 182–195, doi:10.1175/1520-0450(2004)043<0182:ALMAPN>2.0.CO;2, http://journals.ametsoc.org/doi/abs/10.1175/1520-0450(2004)043{%}3C0182:ALMAPN{%}3E2.0.CO;2, 2004.

Scanza, R. A., Mahowald, N., Ghan, S., Zender, C. S., Kok, J. F., Liu, X., and Zhang, Y.: Modeling dust as component minerals in the Community Atmosphere Model: development of framework and impact on radiative forcing, Atmospheric Chemistry and Physics Discussions, 14, 17 749–17 816, doi:10.5194/acpd-14-17749-2014, http://www.atmos-chem-phys-discuss.net/14/17749/2014/, 2014.

Seinfeld, J. H. and Pandis, S. N.: Atmospheric Chemistry and Physics: From Air Pollution to Climate Change, vol. 2nd, Wiley, http://www.knovel.com/knovel2/Toc.jsp?BookID=2126, 2006.

Shipway, B. J.: Revisiting Twomey's approximation for peak supersaturation, pp. 3803–3814, doi:10.5194/acp-15-3803-2015, 2015.

Shipway, B. J. and Abel, S. J.: Analytical estimation of cloud droplet nucleation based on an underlying aerosol population, Atmospheric Research, 96, 344–355, doi:10.1016/j.atmosres.2009.10.005, http://linkinghub.elsevier.com/retrieve/pii/S0169809509002798, 2010.

Simpson, E., Connolly, P., and McFiggans, G.: An investigation into the performance of four cloud droplet activation parameterisations, Geoscientific Model Development, 7, 1535–1542, doi:10.5194/gmd-7-1535-2014, http://www.geosci-model-dev.net/7/1535/2014/, 2014.

Tatang, M., Pan, W., Prinn, R., and McRae, G.: An efficient method for parametric uncertainty analysis of numerical geophysical models, Journal of Geophysical Research, 102, 925–932, http://www.agu.org/pubs/crossref/1997/97JD01654.shtml, 1997.

Topping, D., Connolly, P., and McFiggans, G.: Cloud droplet number enhanced by co-condensation of organic vapours, Nature Geoscience, 6, 443–446, doi:10.1038/ngeo1809, http://www.nature.com/doifinder/10.1038/ngeo1809, 2013.

Twomey, S.: The nuclei of natural cloud formation part II: the supersaturation in natural clouds and the variation of droplet concentration, Pure and Applied Geophysics, http://www.springerlink.com/index/Q0N7L477832V7170.pdf, 1959.

Wang, M., Ghan, S., Easter, R., Ovchinnikov, M., Liu, X., Kassianov, E., Qian, Y., Gustafson Jr., W. I., Larson, V. E., Schanen, D. P., Khairoutdinov, M., and Morrison, H.: The multi-scale aerosol-climate model PNNL-MMF: model description and evaluation, Geoscientific Model Development, 4, 137–168, doi:10.5194/gmd-4-137-2011, http://www.geosci-model-dev.net/4/137/2011/, 2011.

Ward, D. S., Eidhammer, T., Cotton, W. R., and Kreidenweis, S. M.: The role of the particle size distribution in assessing aerosol composition effects on simulated droplet activation, Atmospheric Chemistry and Physics, 10, 5435–5447, doi:10.5194/acp-10-5435-2010, http://atmos-chem-phys-discuss.net/10/4189/2010/acpd-10-4189-2010.pdfhttp://www.atmos-chem-phys.net/10/5435/2010/, 2010.

West, R. E. L., Stier, P., Jones, A., Johnson, C. E., Mann, G. W., Bellouin, N., Partridge, D. G., and Kipling, Z.: The importance of vertical velocity variability for estimates of the indirect aerosol effects, Atmospheric Chemistry and Physics, 14, 6369–6393, doi:10.5194/acp-14-6369-2014, http://www.atmos-chem-phys.net/14/6369/2014/, 2014.

Whitby, K. T.: The physical characteristics of sulfur aerosols, Atmospheric Environment (1967), 12, 135–159, doi:10.1016/0004-6981(78)90196-8, http://linkinghub.elsevier.com/retrieve/pii/S1352231007009739http://linkinghub.elsevier.com/retrieve/pii/0004698178901968, 1978.

Wilson, J., Cuvelier, C., and Raes, F.: A modeling study of global mixed aerosol fields, Journal of Geophysical Research, 106, 34 081–34 108, doi:10.1029/2000JD000198, http://www.agu.org/pubs/crossref/2001/2000JD000198.shtml, 2001.

Yin, Y., Levin, Z., Reisin, T. G., and Tzivion, S.: The effects of giant cloud condensation nuclei on the development of precipitation in convective clouds — a numerical study, Atmospheric Research, 53, 91–116, doi:10.1016/S0169-8095(99)00046-0, http://linkinghub.elsevier.com/retrieve/pii/S0169809599000460, 2000.

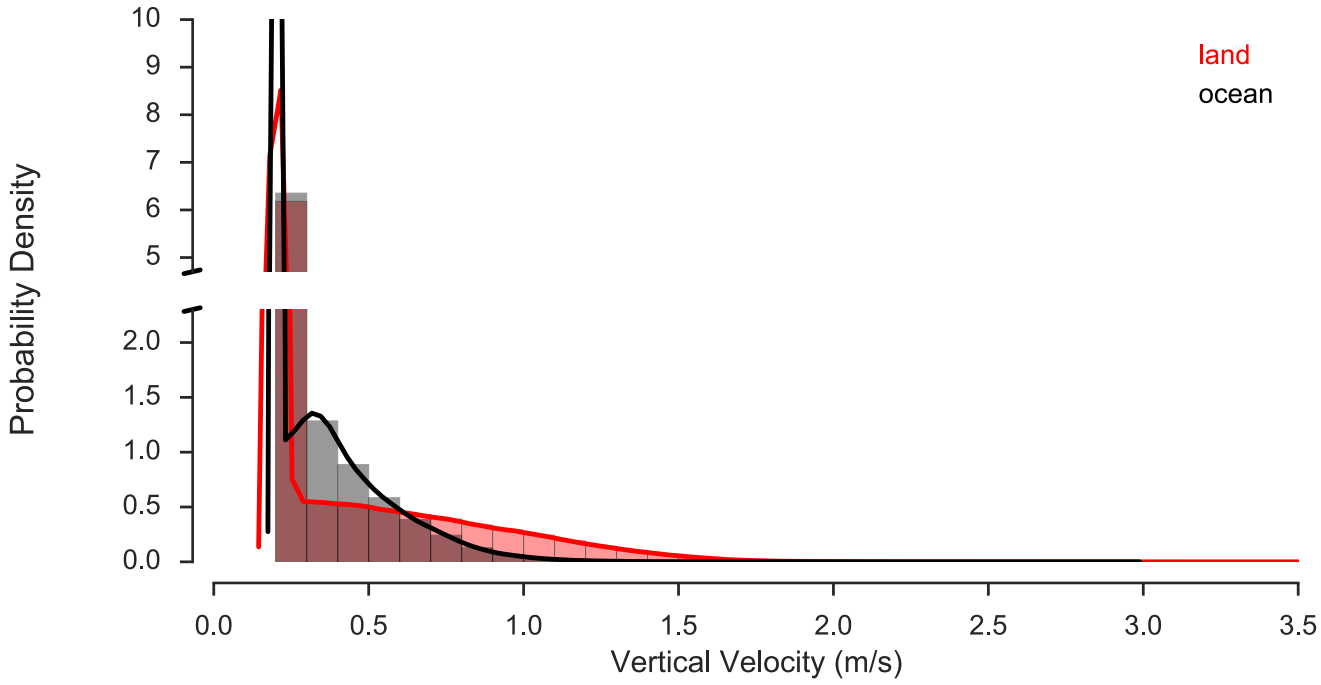

Figure 1. Distributions of model-predicted instantaneous sub-grid scale vertical velocity for near-surface (below 700 mb) grid-cells broken down by land (red) and ocean (black) regimes.

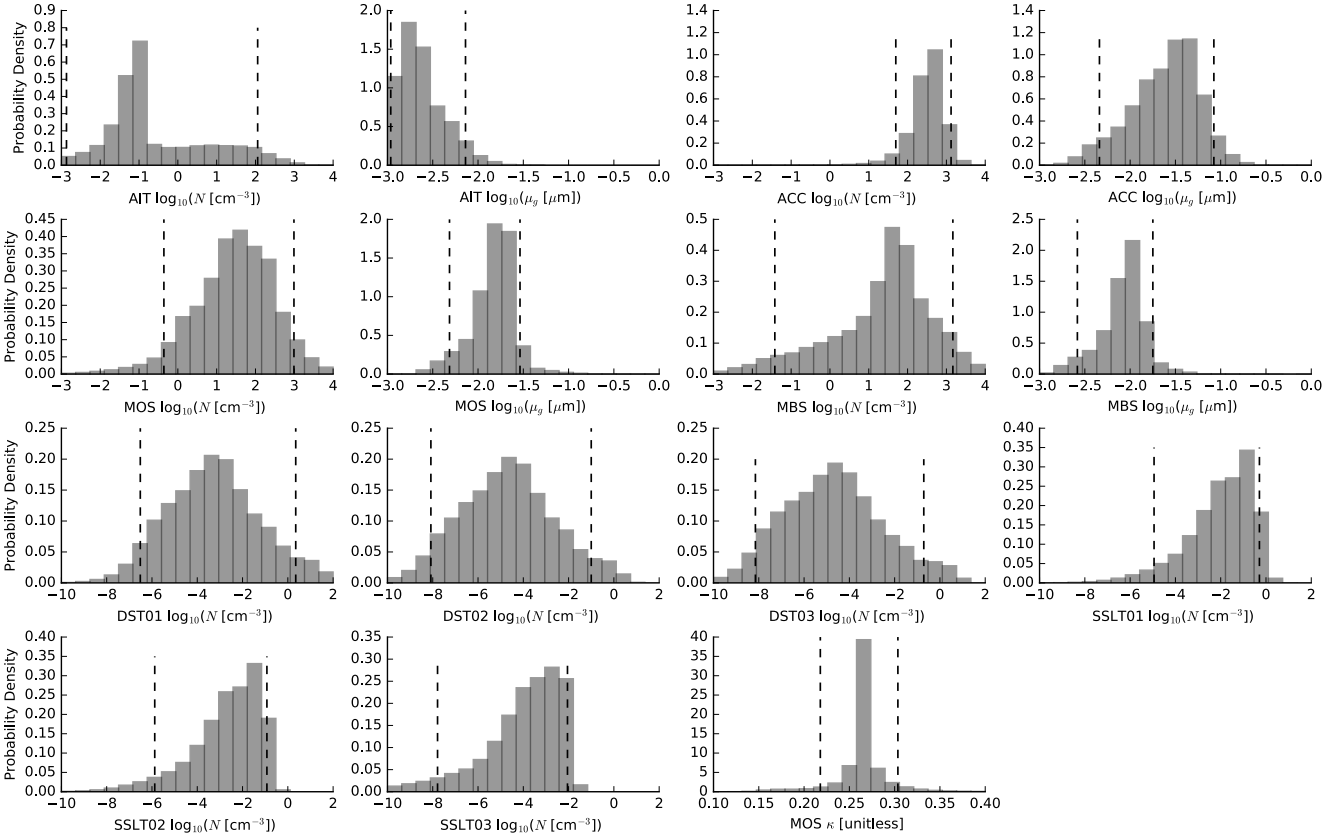

Figure 2. ~~Violinplots showing the distribution~~ Distributions of ~~the logarithm of the number concentration~~ aerosol size distribution parameters for ~~total dust (DST), total sea salt (SSLT), accumulation mode (ACC) and mixed sulfate-black-carbon mode (MBS) aggregated~~ key modes simulated by ~~latitude (columns) and vertical level (rows)~~MARC. ~~The width of each violinplot is scaled by~~ Vertical dashed lines indicate the ~~number~~ 5th and 95th percentiles of ~~observations~~ the sampling distribution for each parameter. Note that each mode name corresponds to those in ~~a given aggregation~~Tables 1 and 2.~~The inner boxplot on each figure shows the median and interquartile range for reference.~~

~~Illustration of particle number, surface area, and mass distributions (left) for typical marine size distribution from Whitby (1978), along with iterative activation calculations (right). In all calculations, we assume the aerosol are all sulfate particles with a hygroscopicity of $\kappa = 0.56$, and are activated in constant-speed updraft of $V = 0.5\,\mathrm{m\,s^{-1}}$~~

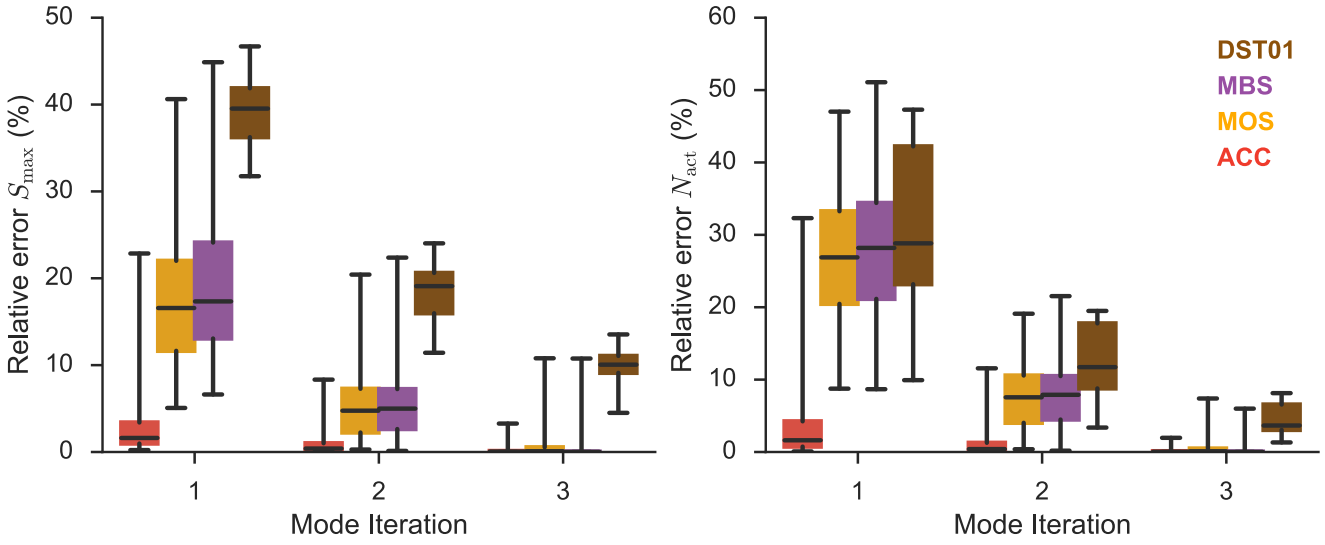

Figure 3. Relative errors in S_{max} (left) and N_{act} (right) in subsequent iterations of the iterative activation calculations. The coloring of each box indicates which mode was the first or dominant one. In each boxplot, box encompasses the interquartile range and the whiskers extend to the 1st and 99th percentiles in the corresponding sub-sample. Outliers beyond these percentiles are not plotted. Labels in legend correspond to accumulation mode (ACC), mixed organic-sulfate mode (MOS), mixed black-carbon sulfate mode (MBS) and smallest dust bin (DST01).

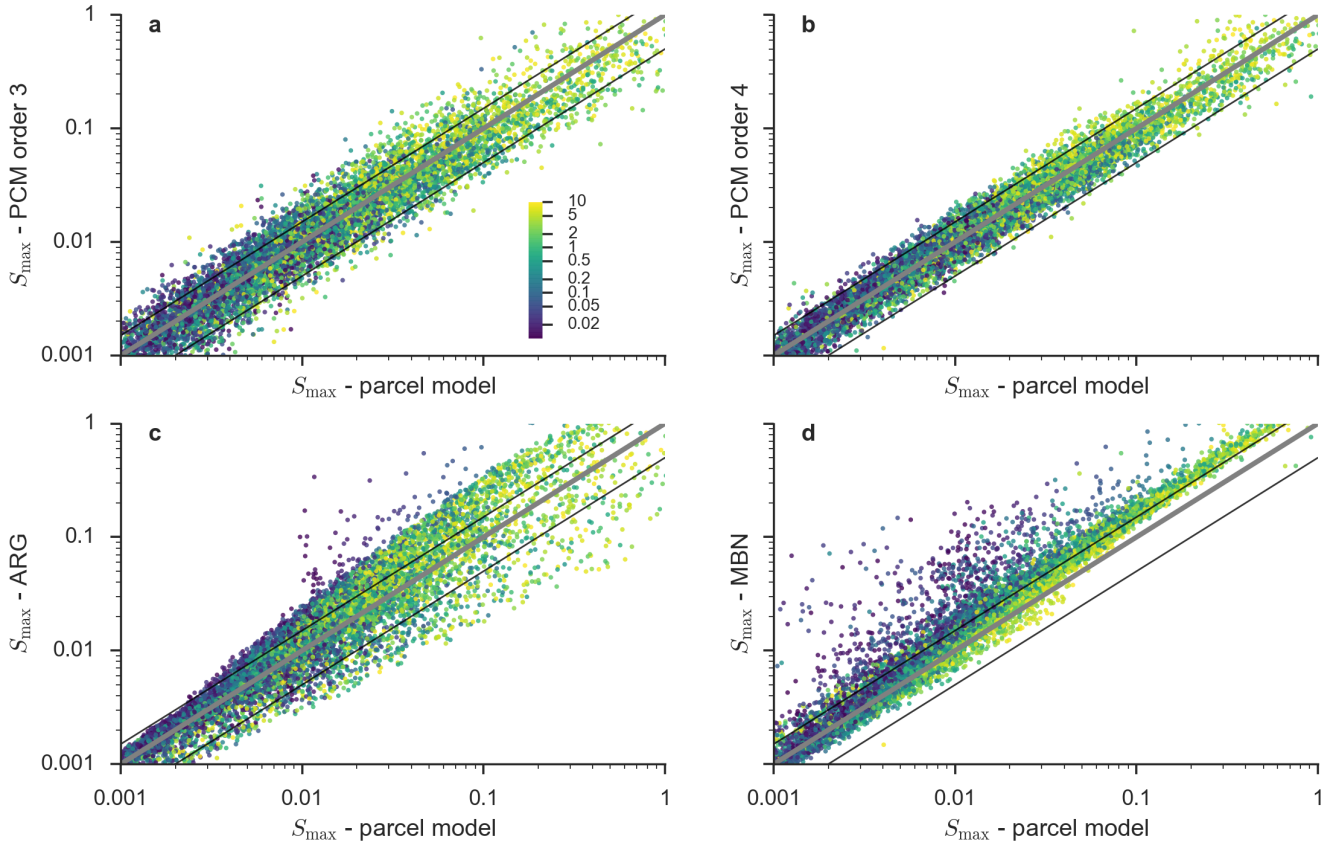

Figure 4. ~~One-one plot comparing predicted~~ Predicted supersaturation maxima ~~between~~ (%)) from parcel model and activation parameterizations - 3rd-order emulator (a), 4th-order emulator (b), ARG (c) and MBN (d). The "main" aerosol parameter set (excluding the dust and sea salt as predictor modes) were utilized here. Glyphs are shaded to denote updraft velocity corresponding to each sample draw (in m/s), and are consistent for each panel. Solid black lines denote a factor-of-2 difference between predicted values from parcel model and corresponding parameterization evaluations

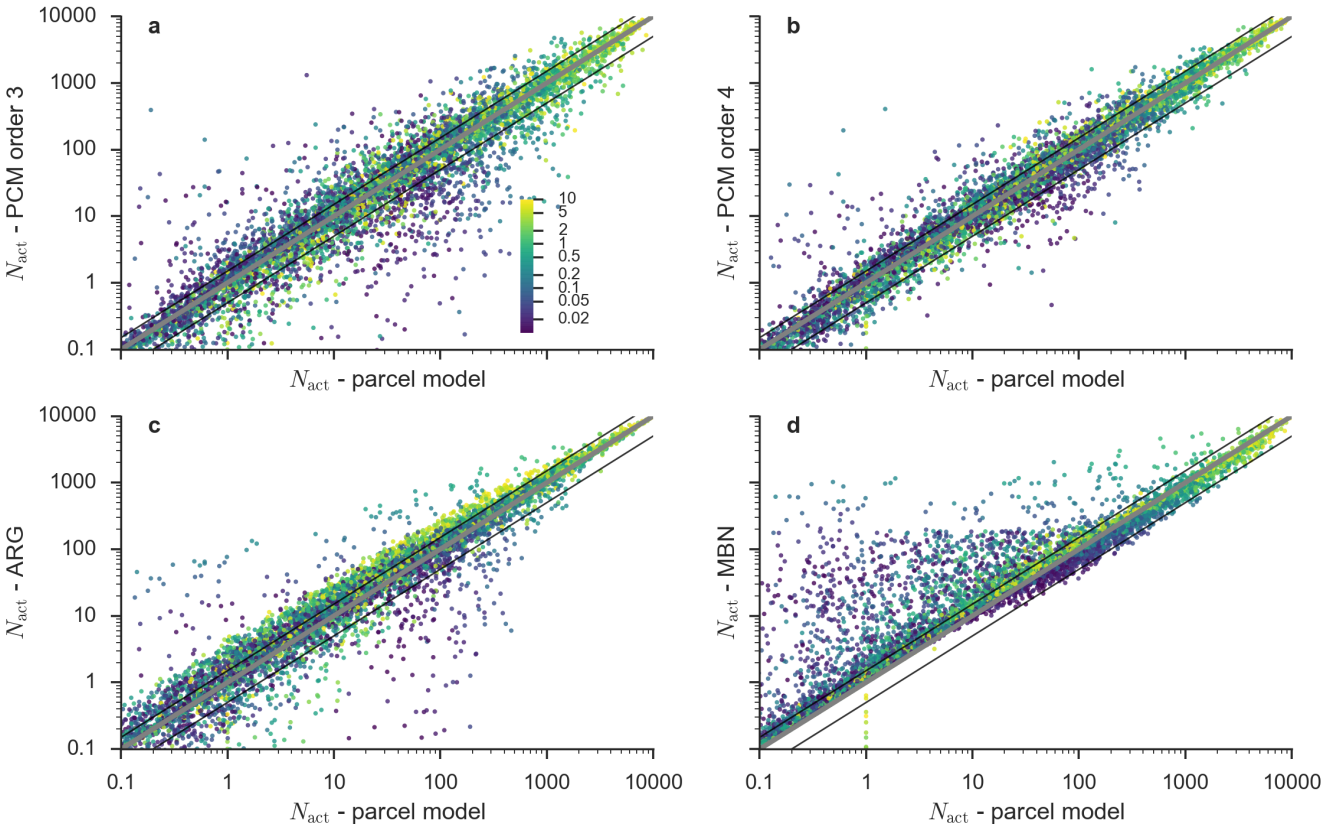

Figure 5. Like Figure 4, but plotting the predicted droplet number concentration (cm^{-3}) nucleated for the aerosol "main" parameter set

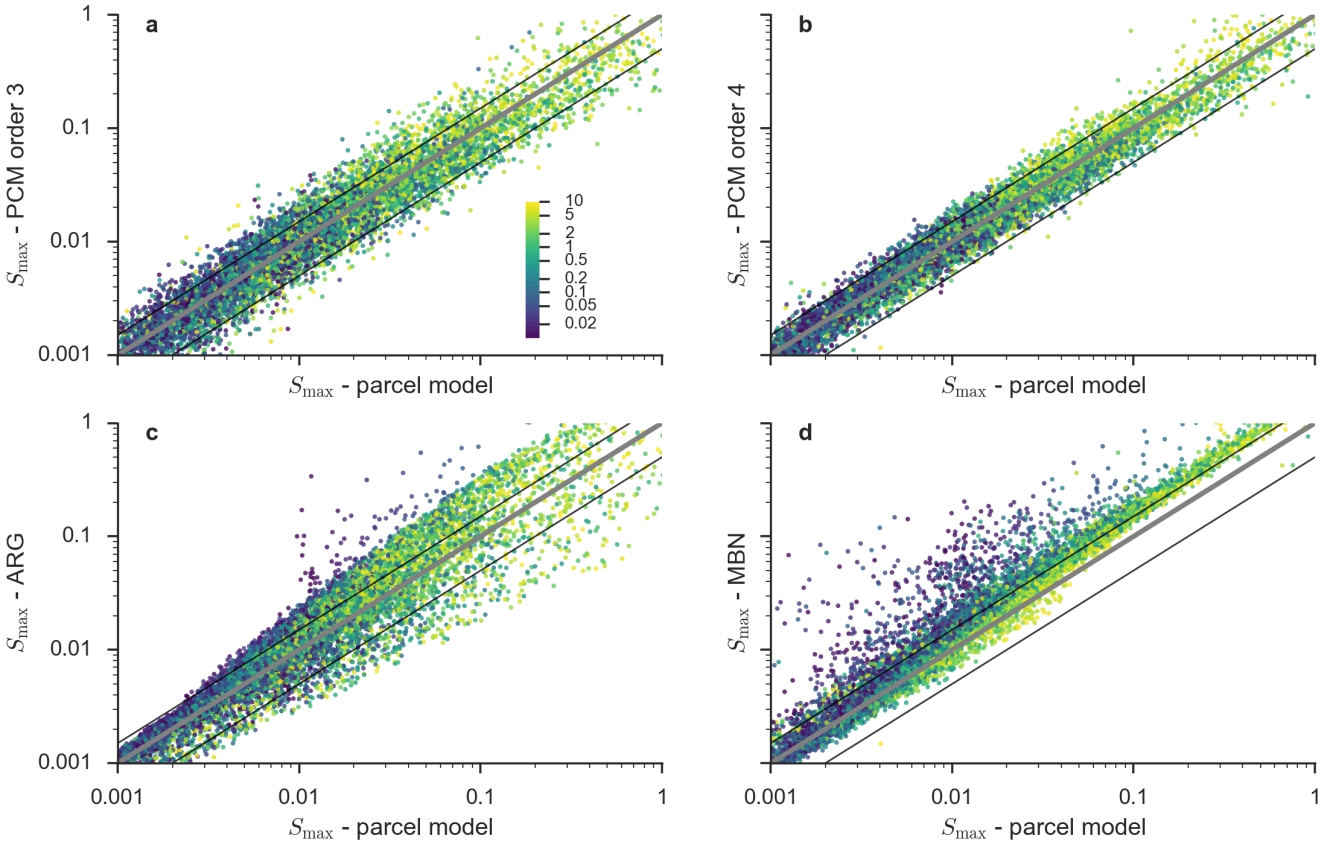

Figure 6. Like Figure 4, but for the "gCCN" parameter set

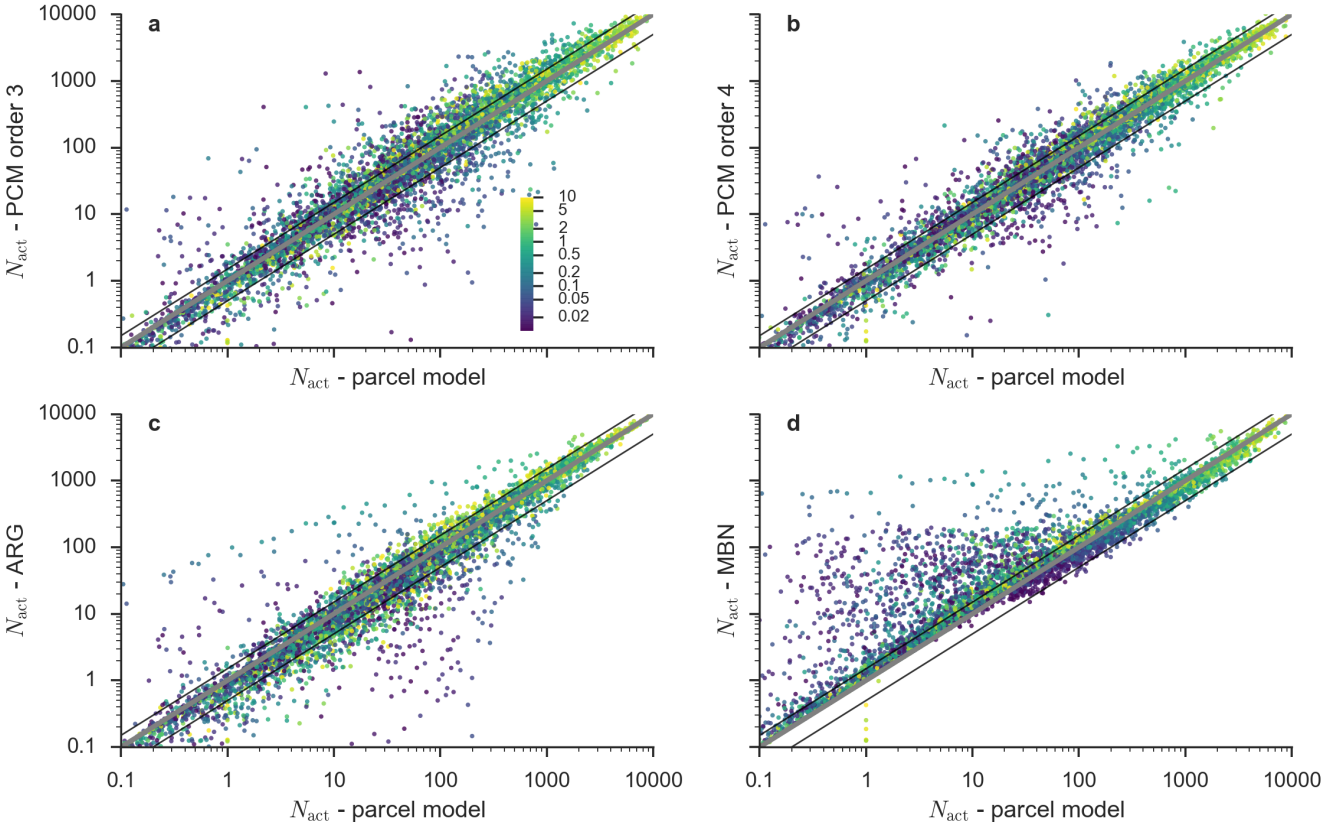

Figure 7. Like Figure 5, but for the "gCCN" parameter set

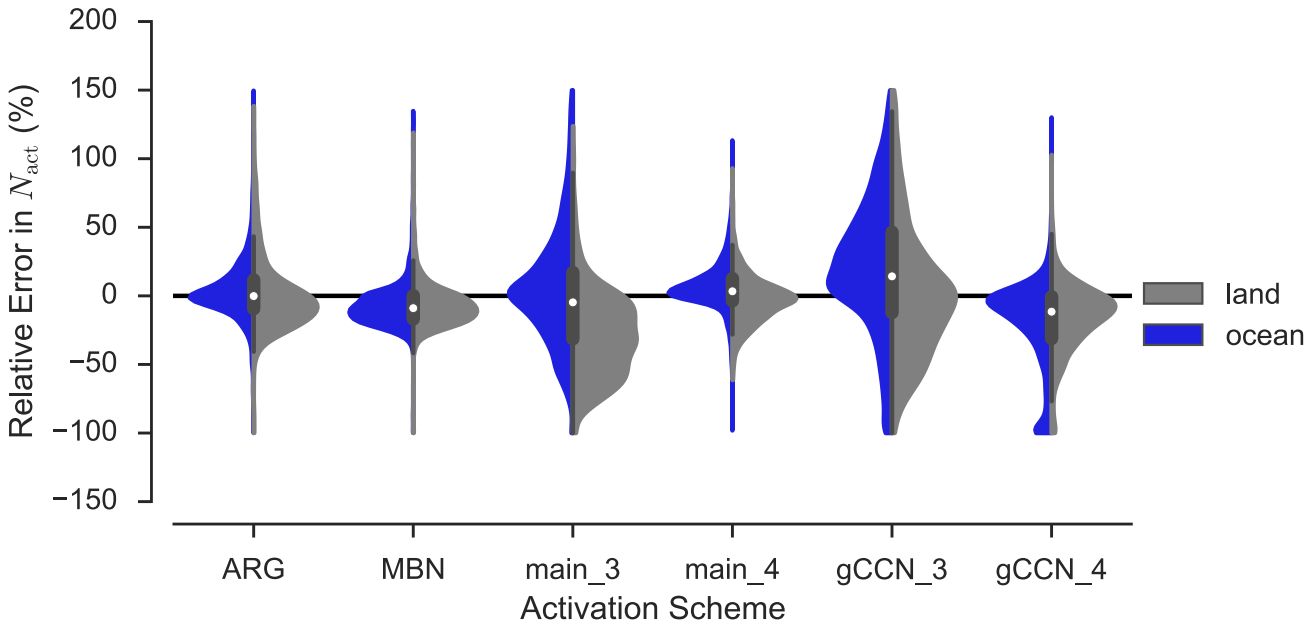

Figure 8. Distributions of relative error in scheme prediction of N_{act} versus detailed parcel, evaluated using samples taken from instantaneous MARC aerosol size distribution and meteorology and colored by geographical regime. The long tail of each distribution is clipped at the extrema for each scheme. The box plot in the center of each distribution shows the median and inter-quartile range of the total distribution of both land and ocean samples for each scheme.

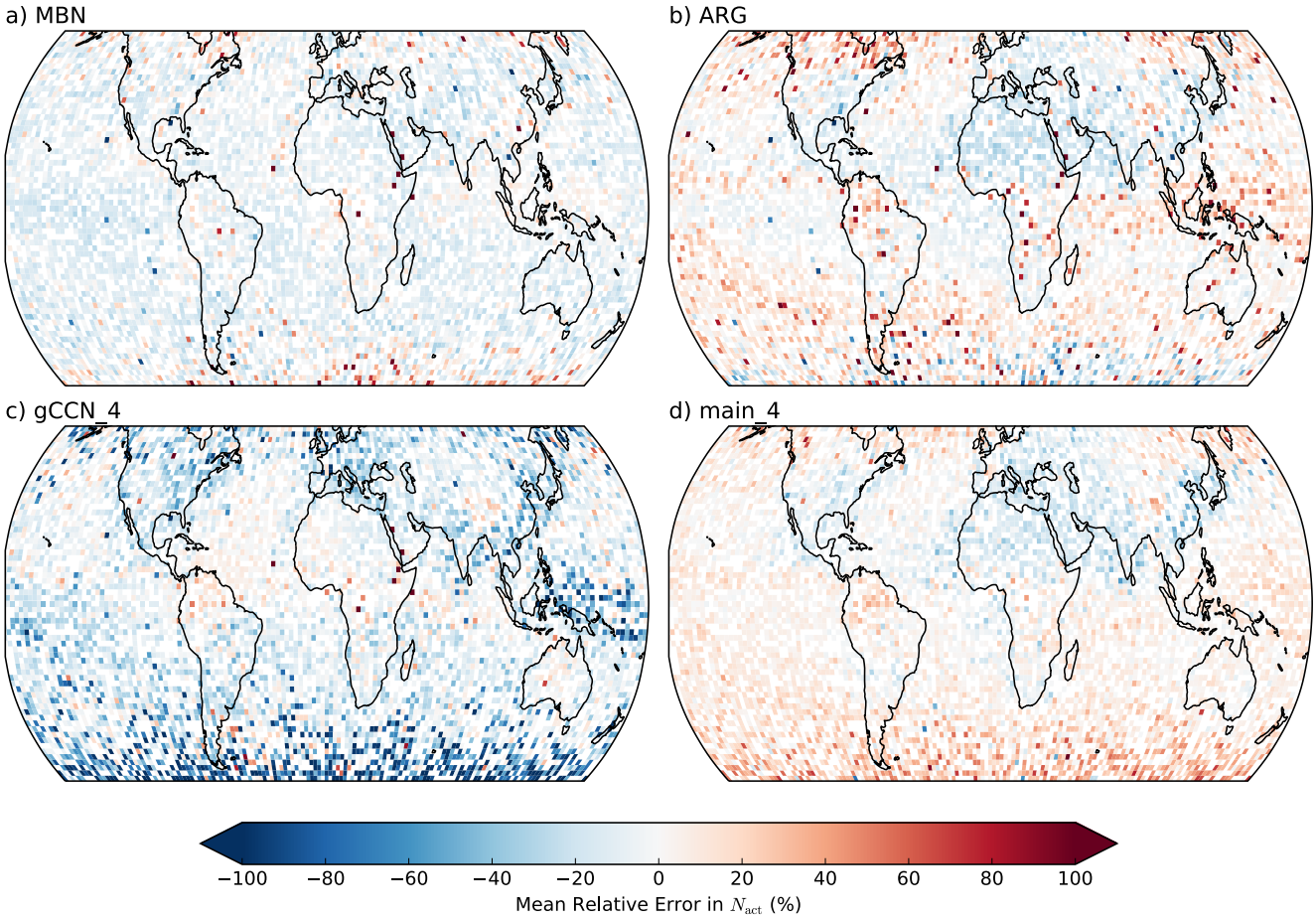

Figure 9. Mean relative error in scheme prediction of N_{act} versus detailed parcel model plotted against location on globe where those samples originated. At each grid location, all samples across timesteps and vertical levels (below 700 mb) are averaged together to compute the mean.

Aerosol Mode	Geometric Mean Particle Diameter (μm)	Geometric Std Deviation (σ_g)	Density ($\mathrm{g\,cm^{-3}}$)	Hygroscopicity (κ)
NUC	0 to 0.005 84	1.59	1.8	0.507
AIT	0.005 84 to 0.031	1.59	1.8	0.507
ACC	>0.031	1.59	1.8	0.507
OC	-	2.0	2.0	10^{-10}
MOS	-	2.0	†	†
BC	-	2.0	2.0	10^{-10}
MBS	-	2.0	2.0	0.507
DST01	0.16	1.4	-	0.14
DST02	0.406	1.4	-	0.14
DST03	0.867	1.4	-	0.14
DST04	1.656	1.4	-	0.14
SSLT01	0.5	1.59	-	1.16
SSLT02	2.0	1.37	-	1.16
SSLT03	5.0	1.41	-	1.16
SSLT04	15.0	1.22	-	1.16

Table 1. MARC aerosol mode size distribution and composition parameters. The MOS mode (†) has a composition-dependent density and hygroscopicity which is computed using the internal mixing state of organic carbon and sulfate present at a given grid-cell and timestep.

Symbol	Description	Lower Bound	Upper Bound
logN_ACC	Log of accumulation mode sulfate number concentration (cm^{-3})	-3 (1.2)	4 (100)
logN_MOS	Log of mixed sulfate-organic carbon number concentration (cm^{-3})	-5 (1.5)	4 (99.9)
logN_MBS	Log of mixed sulfate-black carbon number concentration (cm^{-3})	-5 (1.6)	4 (99.8)
logN_DST01*	Log of 0.16 micron dust particle number concentration (cm^{-3})	-5 (18.2)	2 (99.8)
logN_DST02*	Log of 0.4 micron dust particle number concentration (cm^{-3})	-5 (38.9)	1 (99.9)
logN_SSLT01*	Log of 0.5 micron sea salt particle number concentration (cm^{-3})	-5 (3.6)	1 (100)
logmu_ACC	Geometric mean size of accumulation mode (micron)	-3 (0.1)	0 (98.9)
logmu_MOS	Geometric mean size of mixed sulfate-organic carbon mode (micron)	-3 (0.06)	-1 (98.3)
logmu_MBS	Geometric mean size of mixed sulfate-black carbon mode (micron)	-3 (0.1)	-1 (98.5)
kappa_MOS	Hygroscopicity of mixed sulfate-organic carbon mode	0.1	0.6
log_V	Log of updraft velocity (m/s)	-2	1
T	Temperature (K)	240	310
P	Pressure (Pa)	50000	105000

Table 2. Input parameter space and bounds on associated uniform probability density functions used to derive polynomial chaos expansions for MARC activation. For the lower and upper bounds on the aerosol size distribution parameters, the parenthetical values denote the percentile of the distribution for that parameter at which the bound occurs. All terms are present for the main expansion; terms affixed with an (*) are added for the gCCN expansion.

		$\log_{10} S_{\max}$				N_{act}			
exp	scheme	MAE	MRE	NRMSE	r^2	MAE	MRE	NRMSE	r^2
main	ARG	0.18	-3.26	0.10	0.94	40.14	25.39	0.15	0.98
	MBN	0.20	-11.79	0.18	0.81	59.05	44.95	0.30	0.90
	PCM Order 3	0.16	0.59	0.09	0.95	72.54	9.20	0.31	0.90
	PCM Order 4	0.10	-0.60	0.06	0.98	45.47	8.89	0.19	0.96
gCCN	ARG	0.17	8.54	0.09	0.93	37.41	-3.92	0.15	0.98
	MBN	0.20	-9.58	0.17	0.78	56.03	33.30	0.31	0.89
	PCM Order 3	0.16	0.59	0.08	0.95	81.19	15.14	0.34	0.87
	PCM Order 4	0.10	0.36	0.06	0.98	50.99	6.90	0.23	0.94

Table 3. Summary statistics for error in supersaturation maxima and droplet number nucleated predicted by emulators and activation parameterization relative to corresponding simulations with a detailed parcel model. From left-to-right, each column represents the coefficient of determination (r^2), mean absolute error (MAE), mean relative error (MRE), and the normalized root-mean-square error (NRMSE)

	$\log_{10} S_{\max}$				N_{act}			
scheme	MAE	MRE	NRMSE	r^2	MAE	MRE	NRMSE	r^2
ARG	0.05	-0.16	0.03	0.92	25.5	2.87	0.16	0.94
MBN	0.06	0.05	0.05	0.71	26.7	-6.68	0.19	0.93
main Order 3	0.12	0.42	0.08	0.33	64.7	-1.81	0.44	0.59
main Order 4	0.04	-0.31	0.02	0.96	24	4.59	0.19	0.93
gCCN Order 3	0.14	-1.84	0.09	0.18	75.6	20.9	0.47	0.52
gCCN Order 4	0.12	4.61	0.10	-0.19	44.3	-19.9	0.33	0.76

Table 4. Same as Table 3, but for the sampling study using MARC aerosol and meteorology parameter sets.